International Journal of Greenhouse Gas Control 80 (2019) 103–122

Contents lists available at ScienceDirect

International Journal of Greenhouse Gas Control

journal homepage: www.elsevier.com/locate/ijggc

An integrated geological and GIS-based method to assess caprock risk in mature basins proposed for carbon capture and storage

Chantelle Roelofse[a,*], Tiago M. Alves[a], Joana Gafeira[b], Kamal'deen O. Omosanya[c,d]

[a] 3D Seismic Lab – School of Earth and Ocean Sciences, Cardiff University, CF10 3AT, United Kingdom
[b] British Geological Survey – The Lyell Centre, Research Avenue South, Edinburgh, EH14 4AP, United Kingdom
[c] The Research Centre for Arctic Petroleum Exploration, Norwegian University of Science and Technology, Trondheim, Norway
[d] Oasis Geoconsulting Limited, Nigeria

ARTICLE INFO

Keywords:
Jæren high
Carbon capture and storage
Seal integrity
Fluid flow
Pockmarks
Gas pipes

ABSTRACT

Subsurface injection of carbon dioxide (CO_2) is a technique to enhance oil recovery and so the economic value of depleting fields. It complements carbon capture and storage, which is a key technology to mitigate greenhouse gas emissions. In this work, an integrated method developed by the British Geological Survey and Cardiff University uses high-resolution 3D seismic and borehole data from the Jæren High to analyse potential seal breaches and fluid flow paths in a frontier area of the North Sea, ultimately assessing the risk of a possible carbon capture and storage site. We integrate the spatial analysis of subsurface fluid flow features with borehole and geochemical data to model the burial and thermal history of potential storage sites, estimating the timing of fluid expulsion. On seismic data, fluid pipes connect reservoir intervals of different ages. Spatial analysis reveals clustering of fluid flow features above strata grounded onto deep reservoirs intervals. Our integrated method shows that gas matured from Dinantian coal and migrated up-dip during the Triassic-Jurassic into the lower sandstone reservoir of the Rotliegend Group. The containing seal rock was breached once sufficiently large volumes of gas generated high overpressures in the reservoir. Some of these fluid flow features may still be active conduits, as indicated by bright amplitude anomalies within the pipes. This study shows how integrated analyses may enhance our understanding of fluid-flow pathways, de-risking prospective sites for carbon capture and storage. The method proposed in this work is particularly important to assess the suitability of area with trapped gas pockets and understand tertiary migration in areas proposed for geological storage of CO_2.

1. Introduction

Enhanced hydrocarbon recovery techniques are critical for extracting maximum volumes of hydrocarbons from mature fields. They involve thermal, chemical and gas-injection techniques, one of which comprises the injection of CO_2-enriched solutions in reservoirs approaching depletion (Thomas, 2008). Carbon Capture and Storage (CCS) is itself regarded as an important technique to mitigate CO_2 emissions. This forms a positive feedback in the energy industry since mature basins such as the North Sea contain viable targets for CCS, at the same time benefiting from a vast database of seismic, well and dynamic production data.

In the North Sea, depleted gas fields have been assessed for combined enhanced oil and gas recovery and CCS, e.g. the Bunter Sandstone in the Southern North Sea (Agada et al., 2017; Williams et al., 2013), and the P18-4 Gas Field offshore The Netherlands (Arts et al., 2012). The Utsira Sands, located within the overburden of the Sleipner Gas Field (Norwegian North Sea) have been successful in storing CO_2 for more than 20 years, while natural gas is produced (Eiken et al., 2011). Depleted hydrocarbon fields are particularly important for the implementation of CCS; they can successfully store large volumes of CO_2 as demonstrated by their containment of hydrocarbons over geological timescales. In addition, potential CO_2 storage sites may occur adjacently to known producing fields. One of such cases is the regionally extensive Permian Rotliegend Group, which is a saline aquifer in areas where hydrocarbons are not found in economic volumes (Wilkinson et al., 2013). Notwithstanding the latter example, the injection of CO_2 for combined enhanced hydrocarbon recovery and CCS requires a detailed understanding of geological risks and uncertainties prior to the implementation of such techniques, namely the recognition of potential fluid flow paths through caprocks and the sealing capacity in target storage areas. Previous studies predicting the migration of injected CO_2

* Corresponding author.
E-mail addresses: roelofsec@cardiff.ac.uk (C. Roelofse), alvest@cardiff.ac.uk (T.M. Alves), jdlg@bgs.ac.uk (J. Gafeira), kamaldeen.o.omosanya@ntnu.no (K.O. Omosanya).

https://doi.org/10.1016/j.ijggc.2018.11.007
Received 14 March 2018; Received in revised form 3 October 2018; Accepted 8 November 2018
1750-5836/ © 2018 The Authors. Published by Elsevier Ltd. This is an open access article under the CC BY license (http://creativecommons.org/licenses/BY/4.0/).

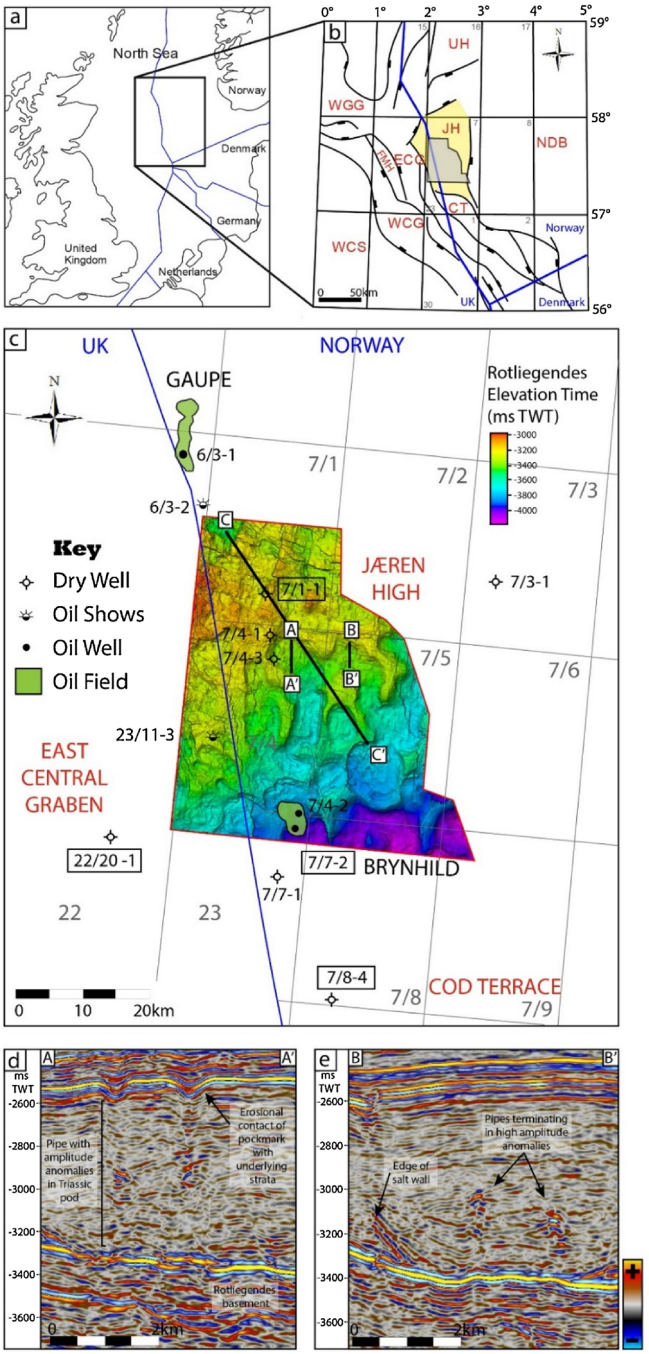

Fig. 1. a) Map of the North Sea. b) Main faults and structural elements near the study area (denoted by the grey polygon); UH = Utsira High; WGG = Witch Ground Graben; FMH = Forties-Montrose High; WCS = West Central Shelf; WCG = West Central Graben; ECG = East Central Graben; CT = Cod Terrace; JH = Jæren High (yellow shaded area); NDB = Norwegian-Danish Basin. Structure was generated from maps provided by the Norwegian Petroleum Directorate. c) Two-way-time elevation surface of the Top Rotliegendes. Key wells and fields are labelled. Well names in boxes are used in the burial history models in Fig. 11. Seismic line C-C' is highlighted in Fig. 5. d) Seismic example of a pipe terminating in a pockmark. e) Seismic example of a pipe terminating in a high-amplitude anomaly. A colour bar is included whereby red and yellow seismic reflections are positive (hard), whilst blue are negative (soft).

plumes have indicated that CO_2 can migrate for large distances. Uncontained CO_2 plumes can reach a large number of nearby wells and create risks in terms of well integrity and gas management in many an oil and gas field (Li et al., 2018).

The study area is located on the Jæren High basement structure; this is a relatively underexplored part of the Norwegian Central North Sea and extends into the UK sector, in which wells target Paleocene successions near large salt diapirs on the eastern margin of the East Central Graben (Fig. 1). In contrast, wells in the Norwegian North Sea penetrate Triassic strata and the Upper Permian Zechstein Group (Fig. 2). Two oil fields have so far been discovered on the Jæren High; the Gaupe Field to the north of the study area and the Brynhild Field to the south (Fig. 1c). Both contain Upper Jurassic reservoirs above broad, developed salt walls. In the study area, pipes and associated depressions are imaged on 3D seismic reflection data within the Mesozoic succession of the Jæren High. These features are likely associated with fluid flow and are rooted in deep Paleozoic strata. Hence, our setting contrasts with salt injection features (Clark et al., 1999) and other documented pipes in the North Sea, which typically originate from Cenozoic strata (e.g. Berndt et al., 2003), or are located above salt diapirs (Salisbury, 1990; de Mahiques et al., 2017).

Pipes are narrow, vertical structures that cross-cut seismic reflections. They consist of high- or low-amplitude seismic anomalies with a columnar geometry in three dimensions (Løseth et al., 2011; Cartwright and Santamarina, 2015). Pipes represent a highly focused fluid-flow path from source to seabed (or paleo-seabed), and indicate that seal integrity has been lost and the seal has been breached (Cartwright et al., 2007).

Throughout this work, the term 'pipe' follows the definition above. In contrast, fluid flow features at the upper terminations of pipes are termed depressions due to their specific morphology; the interpretation of these features is made following the study of their morphology and formation mechanisms. High-amplitude anomalies (bright spots) associated with pipes and depressions may relate to the presence of gas, overpressured strata, local lithological variations and cemented intervals (Løseth et al., 2009). Hence, the aims of this paper are to:

a) Present a novel method to analyse the spatial distribution of buried depressions and pipes by integrating geographic information systems (GIS), seismic and well modelling, using the example of the Jæren High;
b) Determine the timing of fluid flow in the Mesozoic succession of the Jæren High;
c) Relate the presence of fluid flow features to the local and regional geological settings of the UK and Norwegian North Sea;
d) Discuss the implications of seal bypass and associated risks to CCS based on the new method presented here.

Several approaches have been proposed in the literature to characterise areas for carbon capture and storage (CCS), including analytical, semi-analytical, experimental, numerical, and a combination of two or more methods (Crow et al., 2009; Le Guen et al., 2011; Nogues et al., 2012). Geldof et al. (2014) utilised a GIS method for the first time, using 3D seismic data at the seabed level, to study shallow gas migration and subsea geohazards. However, none of the published methods have integrated algorithms embedded in GIS with seismic and petroleum systems data as used in this paper.

2. Geological framework

The stratigraphic framework of the Jæren High is summarised in Fig. 2 and Table 1.

2.1. Paleozoic evolution

The study area is located on the Jæren High, a tilted fault block forming the eastern edge of the East Central Graben (Fig. 1). The Central Graben comprises one of three rift arms of Triassic-Jurassic age, centred 50 km northwest of the Jæren High (Zanella and Coward, 2003). During the Carboniferous widespread peat, fluvial-deltaic sand

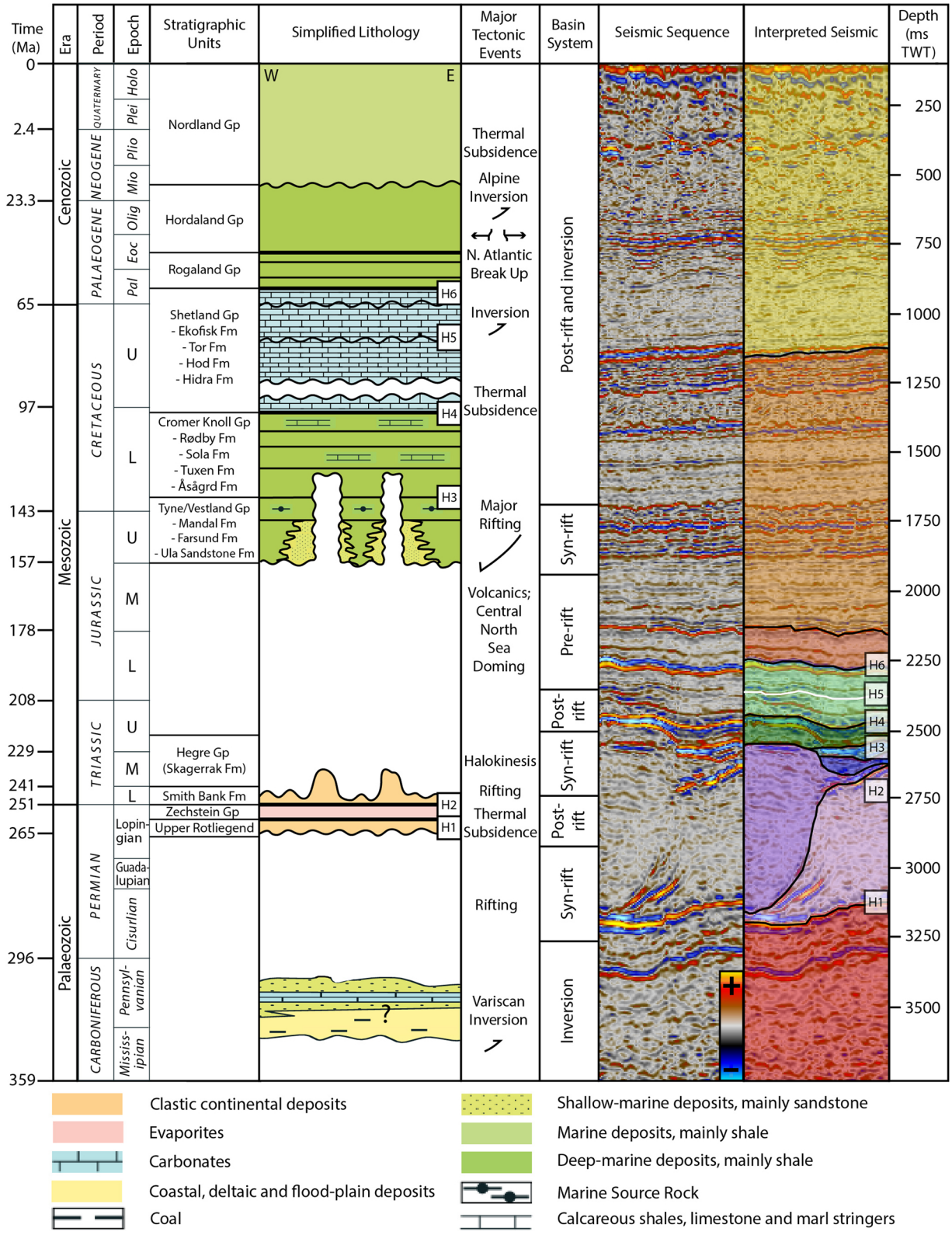

Fig. 2. Stratigraphic framework of the Jæren High. Seismically mapped horizons are denoted as H1 – H6. Representative seismic interpretation is shown on the right. Modified after the Norwegian North Sea Lithostratigraphic Chart from the Norwegian Petroleum Directorate.

and mud were deposited across a broad plain extending south from the Caledonian Highlands of Scotland and Norway towards the Variscan foreland basin (Glennie and Underhill, 1998). The peat deposits converted to coal during subsequent burial. The Variscan Orogeny followed, which originated the E-trending Northern and Southern Permian Basins filled by desert sand and muds of the Rotliegend Group (Glennie, 1998). During the late Permian-earliest Triassic, extension and subsidence of the Permian basins outpaced sedimentation, resulting in sea-level rise and deposition of the evaporitic Zechstein Group (Underhill, 2003) (Fig. 2).

2.2. Mesozoic evolution of the Jæren High

The region returned to a continental setting in the Triassic, a period characterised by active extension (rifting) in semi-arid, intra-continental basins, and halokinesis in areas with thick salt deposits (Goldsmith et al., 2003). This process is described by Penge et al. (1993) and Alves and Elliott (2014) as *rift-raft tectonics*. Subsiding Triassic mini-basins (pods) and adjacent salt walls formed as a result of *rift-rafting*, some of which are 2.3 km high. A positive feedback mechanism ensued until Triassic pods became grounded on the Permian sandstones, forming salt welds. In some cases, the pods were inverted into turtle anticline structures (Karlo et al., 2014). Importantly, grounding of Triassic pods over the Permian strata may have occurred as early as the Middle-Late Triassic on the Jæren High (Smith et al., 1993).

During the Jurassic and Cretaceous, a mantle hot-spot known as the 'North Sea Dome' was present in the region (Underhill and Partington, 1993). This thermal dome caused regional uplift of an area of 2400 km^2 across the Jæren High, promoting important erosion down to Lower Jurassic and Upper Triassic strata (Erratt et al., 1999). Subsequent collapse of the thermal dome marked the onset of Late Jurassic deposition, commencing at the furthest reaches of the grabens and younging towards the centre (Rattey and Hayward, 1993).

2.3. Late Jurassic to Recent evolution

By Late Jurassic time, rifting and transgression outpaced sediment supply, resulting in the deposition of shallow marine sands and deep-marine shales. This occurred initially in isolated, supra-salt minibasins; then homogeneously across the deepest parts of the Jæren High (Høiland et al., 1993). Consequently, Upper Jurassic units on the Jæren High range in thickness from 0 to 200 m, whilst in the adjacent East Central Graben reach up to 1000 m (Fraser et al., 2002).

As active rifting propagated towards the North Atlantic, thermal subsidence resulted in the drowning of the North Sea rift and subsequent deposition of marine sequences of marls, limestones and carbonates during the Early Cretaceous (Cromer Knoll Group; Copestake et al., 2003). In the study area, buried pipes and pockmarks occur in Upper Jurassic-Lower Cretaceous strata, at a depth of 2.5–4 km, revealing episodes of fluid flow during the Mesozoic. Pockmarks were first discovered by King and MacLean (1970) as shallow, crater-like depressions, formed as subsurface water or gas leaked to the seabed, throwing fine sediments into suspension that were dispersed by bottom currents. They have since been widely recorded by multibeam echo-sounders, sidescan sonar and seismic data (e.g. Hovland and Judd, 1988).

Clastic units were reintroduced into the basin in the Paleocene (Ahmadi et al., 2003), leading to the deposition of > 2 km of strata and the (deep) burial of older rift-related sequences. The detailed seismic-stratigraphy of the study area is summarised in Appendix A.

3. Methodology

3.1. Database development

The interpreted 3D seismic reflection data covers an area of 2400 km^2 across the Jæren High. It was provided by PGS (Petroleum Geo-Services) and processed in zero phase, SEG (positive) standard polarity, such that an increase in acoustic impedance with depth manifests as a peak, which is coloured red, whilst a trough is negative and blue (Fig. 2). Bin spacing is 50 x 50 m and the vertical sampling rate is 4 ms. Tuning thickness and lateral resolution of the Mesozoic section approach 50 m, using equations defined by Badley (1985). The main focus of this study is the Mesozoic section, from 2 to 4.3 s two-way travel time (TWT).

Wireline logs and reports of twelve exploration wells were used, of

Table 1
Summary of the stratigraphy of the Jæren High and seismic units mapped.

Age of Base	Stratigraphic Units	Thickness (m)	Seismic Units	Seismically Mapped Horizon Number	Lithological Character
Paleocene	Nordland, Hordaland & Rogaland Groups	1800 - 2600			Hemipelagic marine shales with interbedded thin sand bodies.
Early-Late Cretaceous	Chalk Group	300 - 500	Top Chalk Group Intra-Chalk Group	H6	Chalk limestone unit.
				H5	Chalk limestone unit.
Early Cretaceous	Cromer Knoll Group	20 - 250	Top Cromer Knoll Group	H4	Calcareous claystones and marlstones.
Late Jurassic	Mandal Formation	0 - 200	Top Mandal Formation	H3	Predominantly deep marine, organic-rich shales (Mandal Formation).
	Ula Formation				The Ula Formation consists of shallow marine sandstones, but is mostly sub-seismic.
Latest Permian	Skagerrak Formation	0 - 2300			Skagerrak Formation: interbedded fluvial sandstone and mudstone successions.
	Smith Bank Formation				Smith Bank Formation: dominated by lacustrine and floodplain mudstones, with minor interbedded siltstone units.
Late Permian	Zechstein Group	0 - 2300	Top Zechstein Group	H2	Evaporite succession consisting of interbedded halite, anhydrite, and minor carbonate and dolomite stringers.
Permian	Rotliegend Group	200 - 500	Top Rotliegend Group	H1	Red, aeolian sandstone unit, with minor interbedded, fine grained desert lake and sabkha facies.
Late Devonian	Carboniferous units	1000 +			A mixture of coal, fluvial-deltaic sand and mudstones.

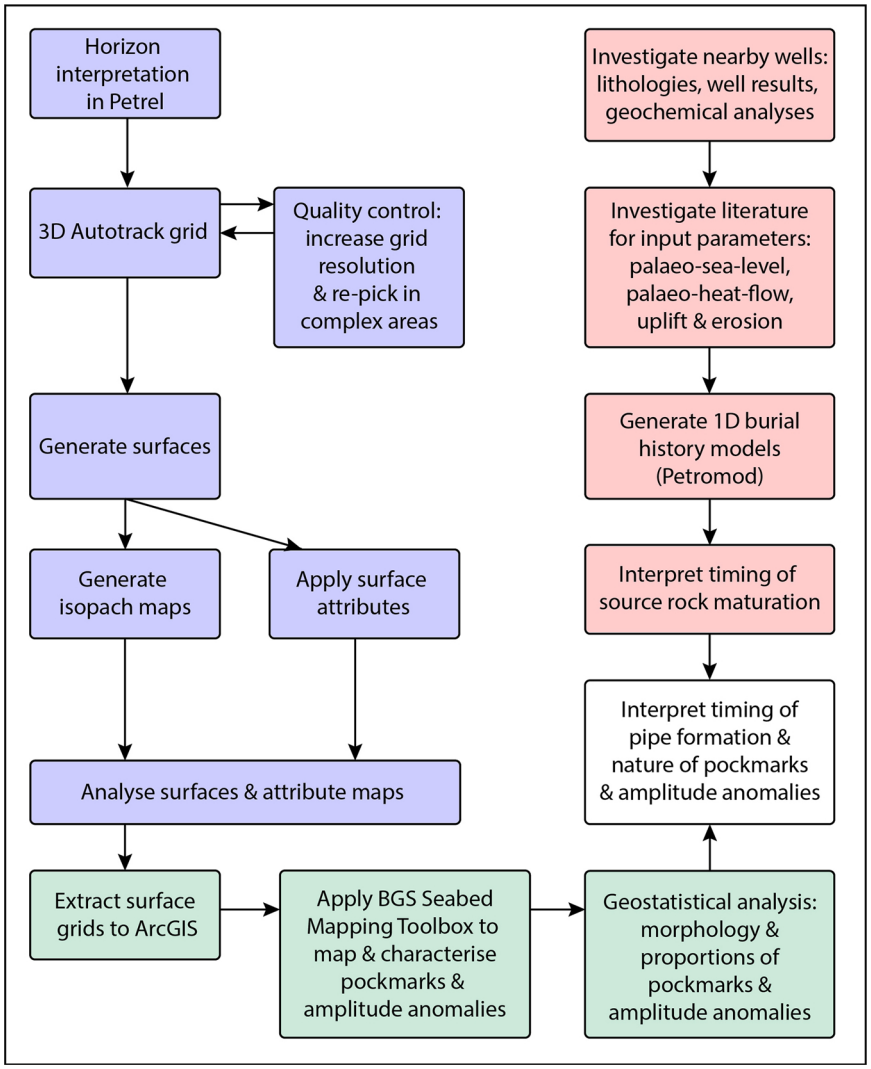

Fig. 3. Flow chart summarising the methodology used in this study. Three different types of software were used; Petrel® for seismic interpretation (blue boxes); ArcGIS® for mapping pockmarks and anomalies (green boxes), as well as spatial and morphological analysis of mapped features, and Petromod® for the maturation modelling of key wells (red boxes).

which two were provided by the British Geological Survey for the UK sector. Detailed well information including composite logs, well reports and geochemical reports of the remaining ten wells were obtained from the Norwegian Petroleum Directorate online database.

3.2. Seismic interpretation

Schlumberger's Petrel® was used to interpret the seismic and well data. The adopted methodology is summarised in Fig. 3. Six horizons (H1 to H6) were mapped on seismic data to highlight the pod-interpod structure of the Mesozoic succession and the associated distribution of buried pockmarks (Figs. 2 and 6). Five wells were tied to the seismic data to correlate horizons and constrain the local stratigraphy, of which three wells (6/3-2, 7/1-1 and 7/7-2) are shown in Fig. 4. Isopach maps were generated from interpreted surfaces to highlight lateral thickness changes and the distribution of salt walls and welds.

3.3. Seismic attributes

Volume and surface attributes in Petrel were used to constrain and visualise fluid flow features in the 3D seismic volume. Variance (or coherence) is a measure of the waveform similarity, recording how similar a given trace is to its neighbouring trace. Similar traces are mapped as low variance values, while discontinuities have high variance values (Brown, 2011). The variance attribute highlights irregularities such as faults, depressions, chaotic pipe interiors and salt walls. The surface attribute 'Maximum Magnitude' extracts the maximum positive or negative seismic amplitude value between two horizons or a time window (Omosanya and Alves, 2013; Marfurt and Alves, 2014).

Maximum Magnitude maps were extracted between the interpreted Mesozoic surfaces to determine whether any high-amplitude anomalies were prevalent – possibly representing fluid pockets or cemented units – and if there is any spatial significance to them (Fig. 5). However, not all the high-amplitude anomalies in the Triassic pods were extracted initially, as they have similar or lower amplitudes to high-amplitude strata in the Skagerrak Formation where this latter is present immediately (down to 150 ms TWT) below horizon H4 (Top Cromer Knoll Group; Figs. 5 and 8). Equally, the extent of any high-amplitude anomalies observed immediately below the pockmarks cannot be mapped clearly if they are similar in amplitude to the more continuous seismic reflections in the Skagerrak Formation. To overcome these limitations, the anomalies within 150 ms TWT below horizon H4 (Top Cromer Knoll Group) were mapped manually on Petrel®, and their presence was assigned to the attribute tables of depressions that coincide with seismic anomalies (Table 2). Secondly, the window for Maximum Magnitude extraction was reduced to between 150 ms TWT

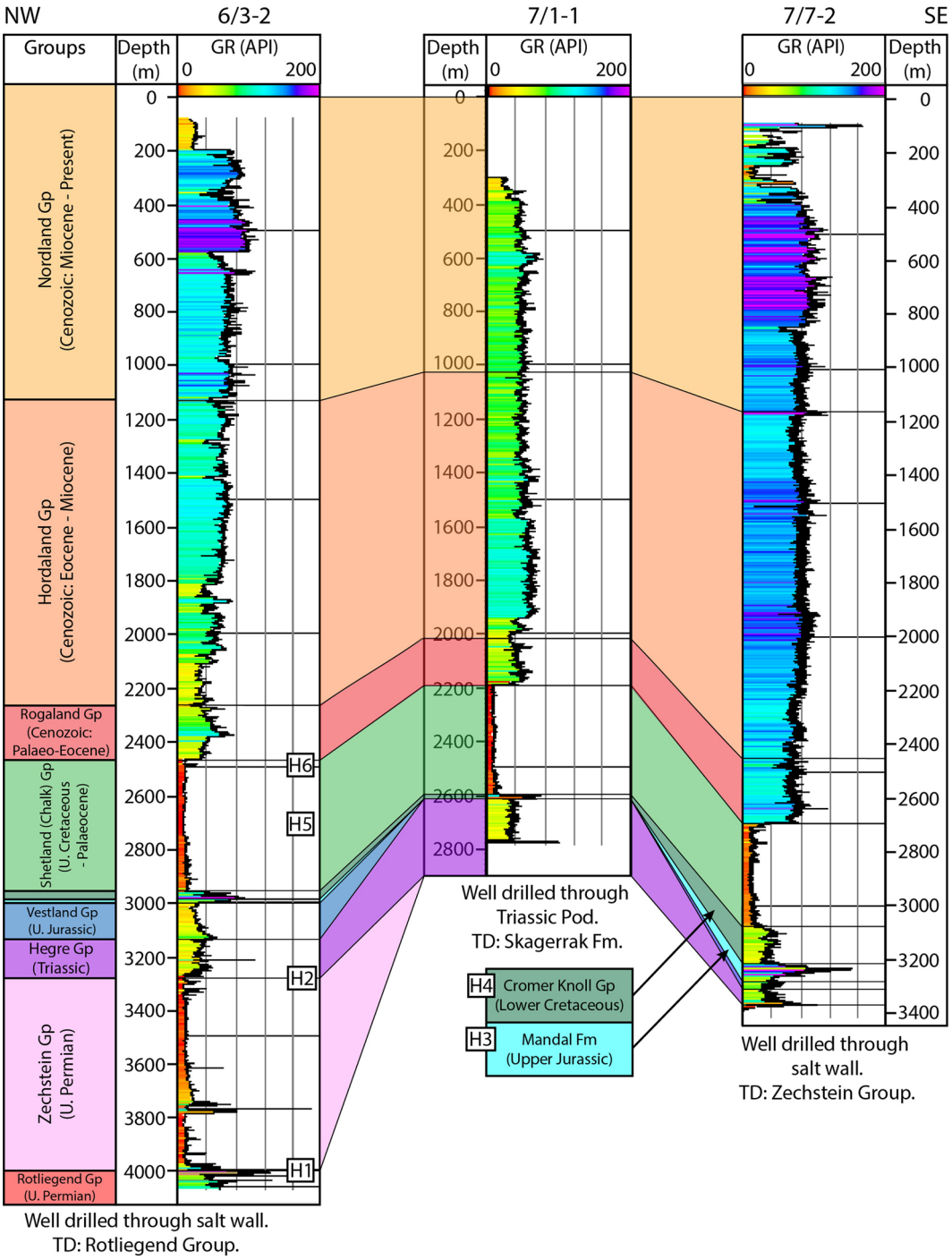

Fig. 4. Well correlation panel using gamma ray logs, from the northwest (6/3-2) to southeast (7/7-2), through salt walls and a Triassic pod. The seismic horizons mapped in this work are named H1 to H6.

below the Top Cromer Knoll Group (horizon H4), and 50 ms TWT above the Top Salt horizon H2, thus reducing any spurious results due to human error when mapping the Top Salt Horizon (Fig. 5). The resulting Maximum Magnitude surface was then exported to ArcGIS and the high-amplitude anomalies were identified using the semi-automated mapping tool developed by the British Geological Survey, described below.

3.4. ArcGIS semi-automated mapping and characterisation

Three seismic surfaces containing circular depressions were exported from Petrel into ArcGIS® version 10.1: the Top Mandal Formation (H3), Top Cromer Knoll Group (H4) and Intra-Chalk (H5) (Fig. 4). An ArcGIS-based Toolbox developed by the British Geological Survey – the BGS Seabed Mapping Toolbox (Gafeira et al., 2012, 2018) – was used to semi-automatically map the confined depressions within each horizon and extract morphological characteristics that include Vertical Relief, Width, Length and Width:Length Ratios, and distribution of depressions. The depressions were mapped automatically by the Toolbox; however, manual interpretation is required to quality-control the automatic mapping. The Toolbox was first used for delineating pockmarks in multibeam echosounder data (Gafeira et al., 2012), and once in 3D seismic data (Geldof et al., 2014), but only at the seabed and 150 ms TWT below the seabed.

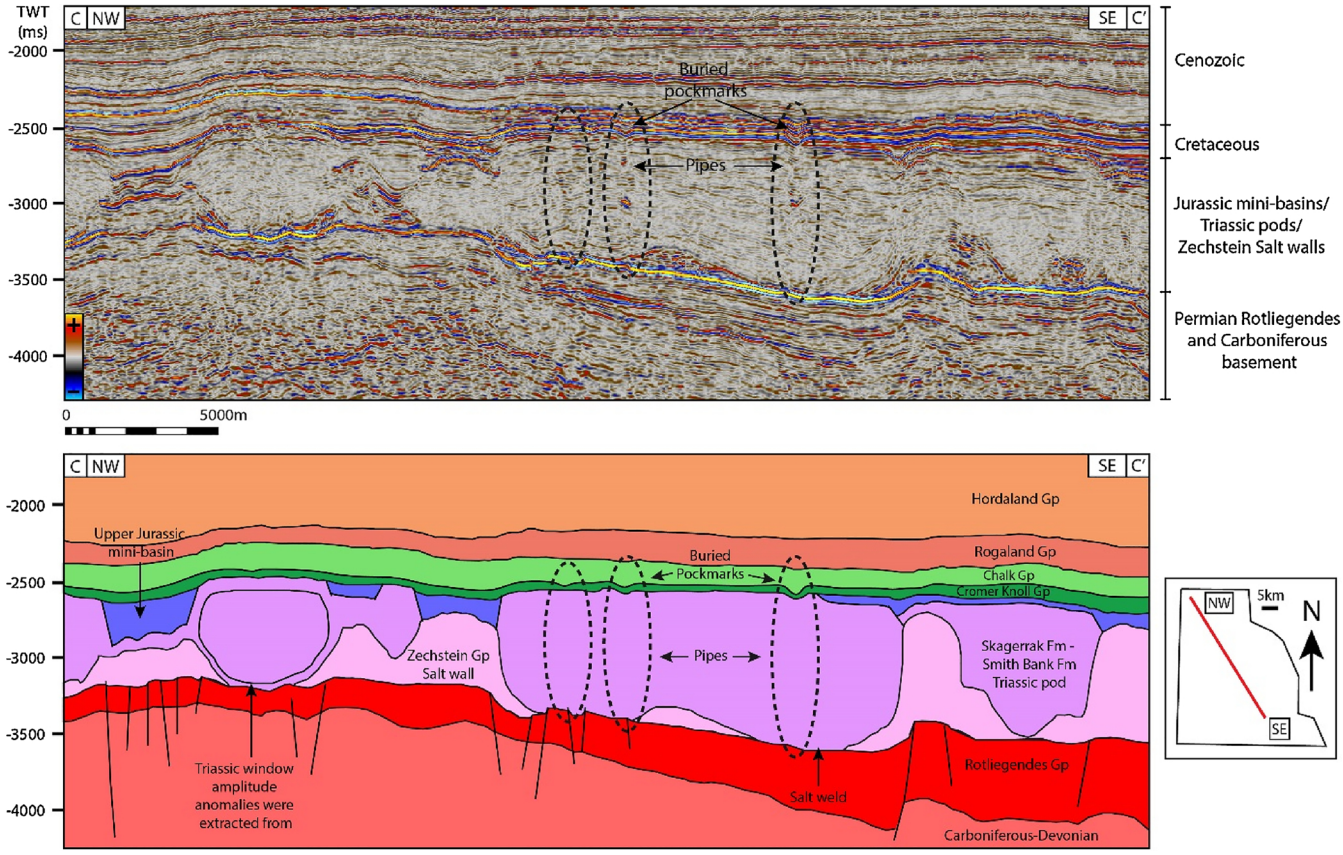

Fig. 5. Regional seismic line between -1800 ms TWT and -4200 ms TWT, from northwest to southeast, showing the key features of the Jæren High: faulted and tilted basement, salt walls and grounded sediment pods crosscut by vertical pipes that terminate in buried pockmarks. The Triassic window for maximum magnitude extraction of high-amplitude anomalies is also highlighted.

The Toolbox mapping thresholds described in Gafeira et al. (2012) (*Minimum Vertical Relief, Minimum Width* and *Minimum Width:Length Ratio*) were adapted for this dataset. The *Minimum Vertical Relief* was defined as 25 m, half of the vertical resolution. The horizontal resolution is 50 m; as a geometric shape must be defined by at least 2 pixels, the *Minimum Width* was chosen to be 100 m, whilst the *Minimum Width:Length ratio* was 0.2, as used in Gafeira et al. (2012).

The morphological characteristics are used to compare the mapped depressions with the published data and to interpret possible mechanisms for their formation. High-amplitude anomalies in Triassic basins (pods) were also delineated by polygons in ArcGIS® using this mapping Toolbox, although further manual interpretation was required to compare them with the depressions as some high amplitudes are due to lithological variations. The width of both depressions and acoustic anomalies was defined using the ArcGIS minimum bounding geometry function. This function computes a rectangle defining the smallest area enclosing the delineated depressions and acoustic anomalies, which is used to infer pockmark eccentricity and ellipse axes lengths (Geldof et al., 2014). The Width and Width:Length Ratio of the acoustic anomalies, as well as the pipe height, were assigned to the ArcGIS attribute table describing the depressions.

In order to obtain the morphological characteristics of depressions, interpreted surfaces had to be converted from two-way time to the depth domain. Interval velocities were obtained from wells from the nearby Brynhild and Gaupe fields (Fig. 1) and used to depth-convert the interpreted seismic volume in Petrel®.

Spatial analysis was conducted visually by overlaying the delineated depressions and anomalies above the salt isopach surface. Statistical data was computed based on the BGS Seabed Mapping Toolbox by plotting box plots, calculating percentages of depressions in different settings, and plotting data on scatter graphs.

3.5. Geochemical analysis and basin modelling

Schlumberger's Petromod® was used to generate simplified, 1D burial history plots. Model inputs such as sub-surface lithologies, thicknesses, ages and bottom-hole temperatures were derived from well reports from the Norwegian Petroleum Directorate database. The magnitude and timing of tectonic uplift events, as well as a palaeo-sea level curve, were obtained from the literature (e.g. Ziegler, 1992; Underhill and Partington, 1993; Monaghan et al., 2017). The thermal history used was taken from Frederiksen et al. (2001). Although the thermal history in this latter work is characteristic of strata further to the south of the Jæren High, it was considered as representing the regional heat flow values for the study area. Model parameters are summarised in Appendix B.

The thickness of strata not penetrated by wells, such as Zechstein, Rotliegendes and Carboniferous strata, are estimated from the depth-converted seismic volume and by using interval velocities from exploration wells 7/3-1 and 6/3-2. The interpretations in Milton-Worssell et al. (2010) also provided valid constraints on the thickness of Paleozoic strata.

Pepper and Corvit (1995) ran a series of experiments to redefine the hydrocarbon generation windows for different organofacies, from marine shale source rocks to terrestrial, humic coal source rocks. They concluded that for humic coals such as the Westphalian in the Southern North Sea, the gas generation window ranges from 175 °C to 220 °C to generate between 10% and 90% of the potential gas in Paleozoic source rocks. The oil generation window for a marine shale source such as the Kimmeridge Clay Formation (UK equivalent of the Mandal Formation in the Norwegian North Sea) ranges from 105 °C to 145 °C, and its gas generation window varies from 145 °C to 210 °C. These isotherm thresholds for the two source rocks are labelled on the resulting burial

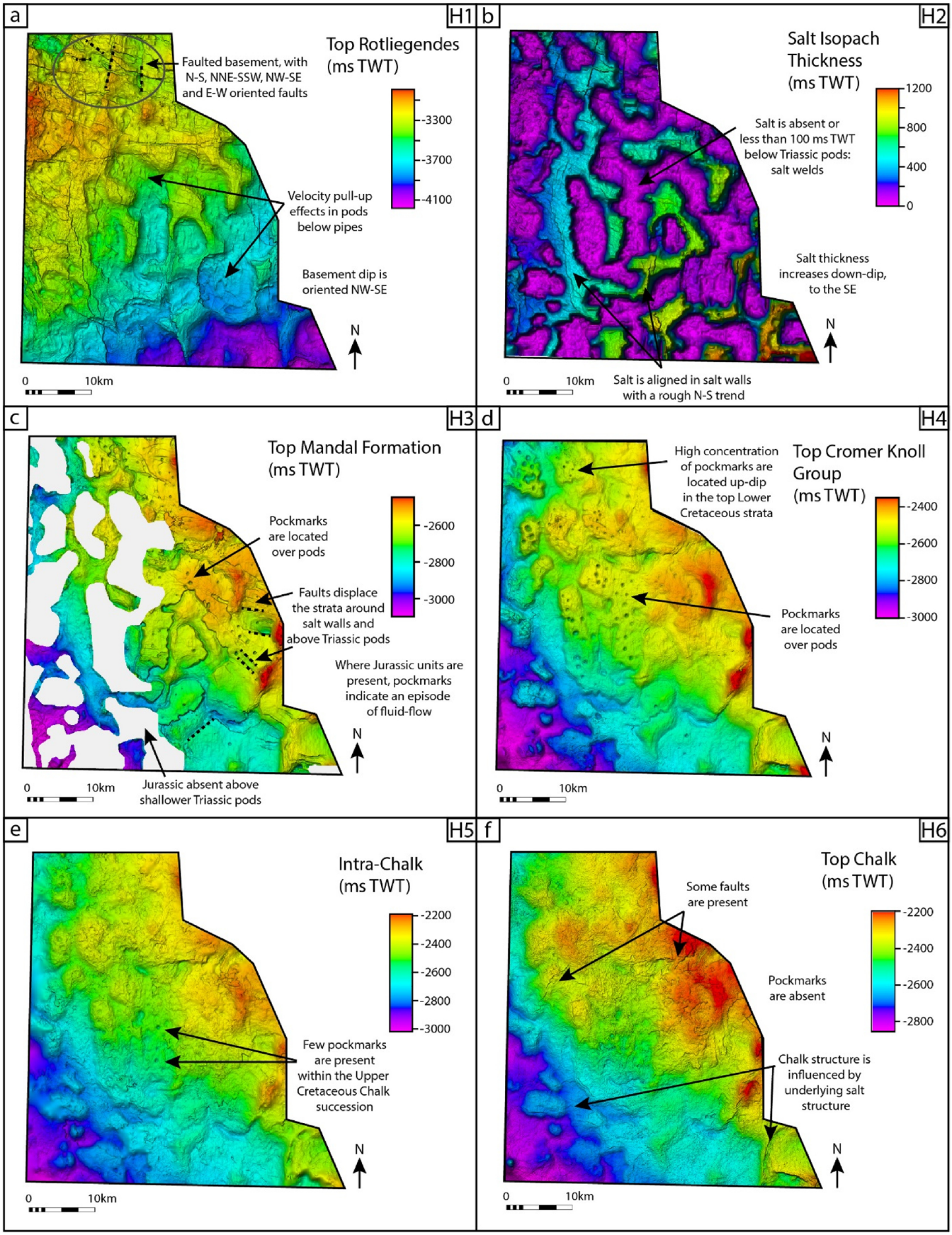

Fig. 6. Two-way time structural maps of key horizons mapped in the study area, with key structural features such as faults and fluid flow features labelled in the figure. a) Time-structural map for the Top Rotliegendes (horizon H1). b) Two-way time salt isopach map showing salt walls. Salt welds are observed where salt is absent or below ~100 ms TWT. c) Time-structural map for the Top Mandal Formation (horizon H3). d) Time-structural map for the Top Cromer Knoll Group (horizon H4). e) Time-structural map for the Intra-Chalk Group horizon H5. f) Time-structural map for the Top Chalk Group (horizon H6).

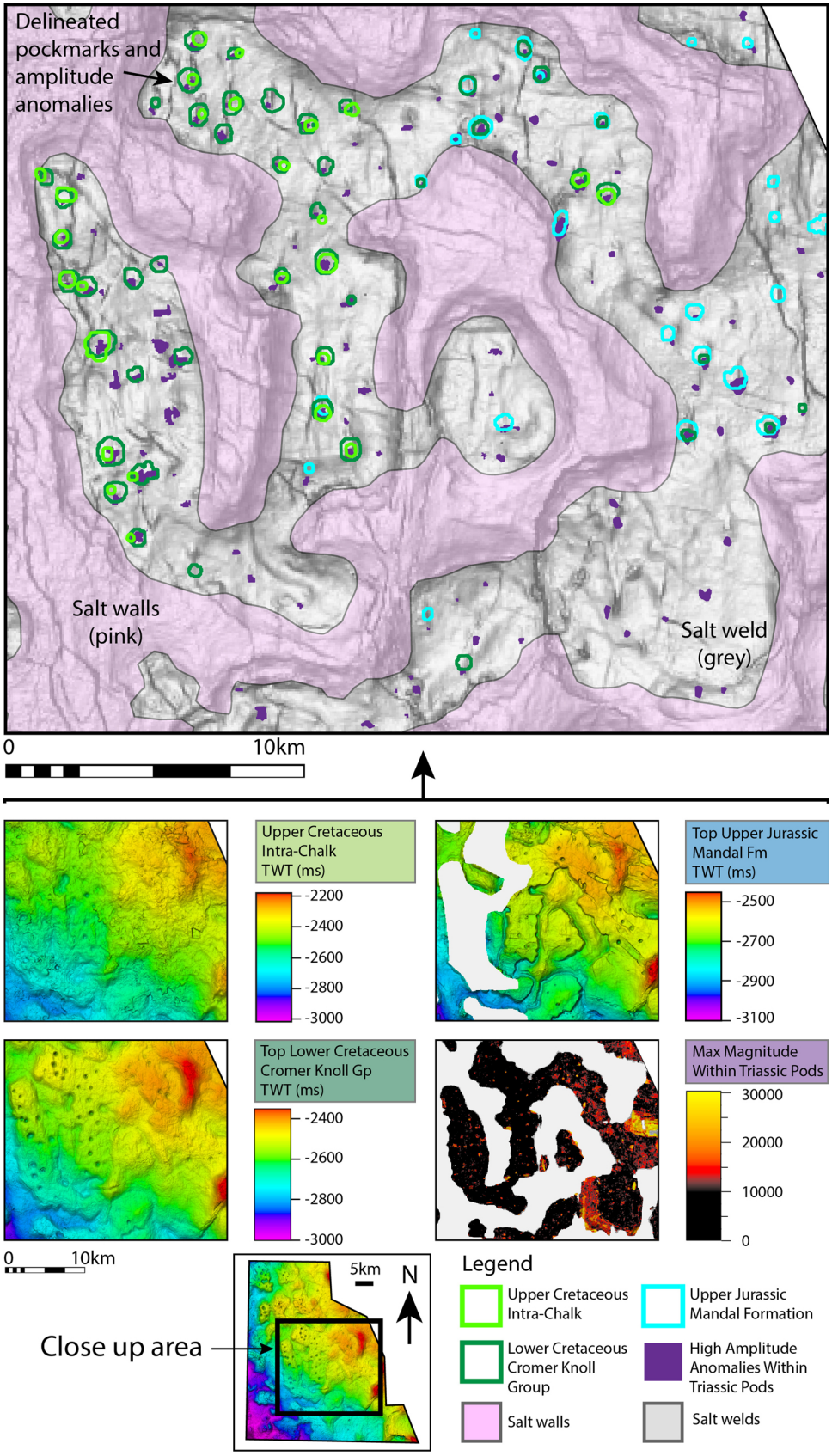

Fig. 7. Depressions and amplitude anomalies delineated in ArcGIS®. Open polygons denote mapped depressions, closed purple polygons denote mapped amplitude anomalies. The basemap shows the variance attribute from the Top of the Rotliegend Group (Horizon 1), highlighting the presence of multiple basement faults (dark grey). It is clear from superimposing the mapped polygons with the salt that depressions and anomalies are only distributed within the Triassic pods *(For interpretation of the references to colour in this figure legend, the reader is referred to the web version of this article).*

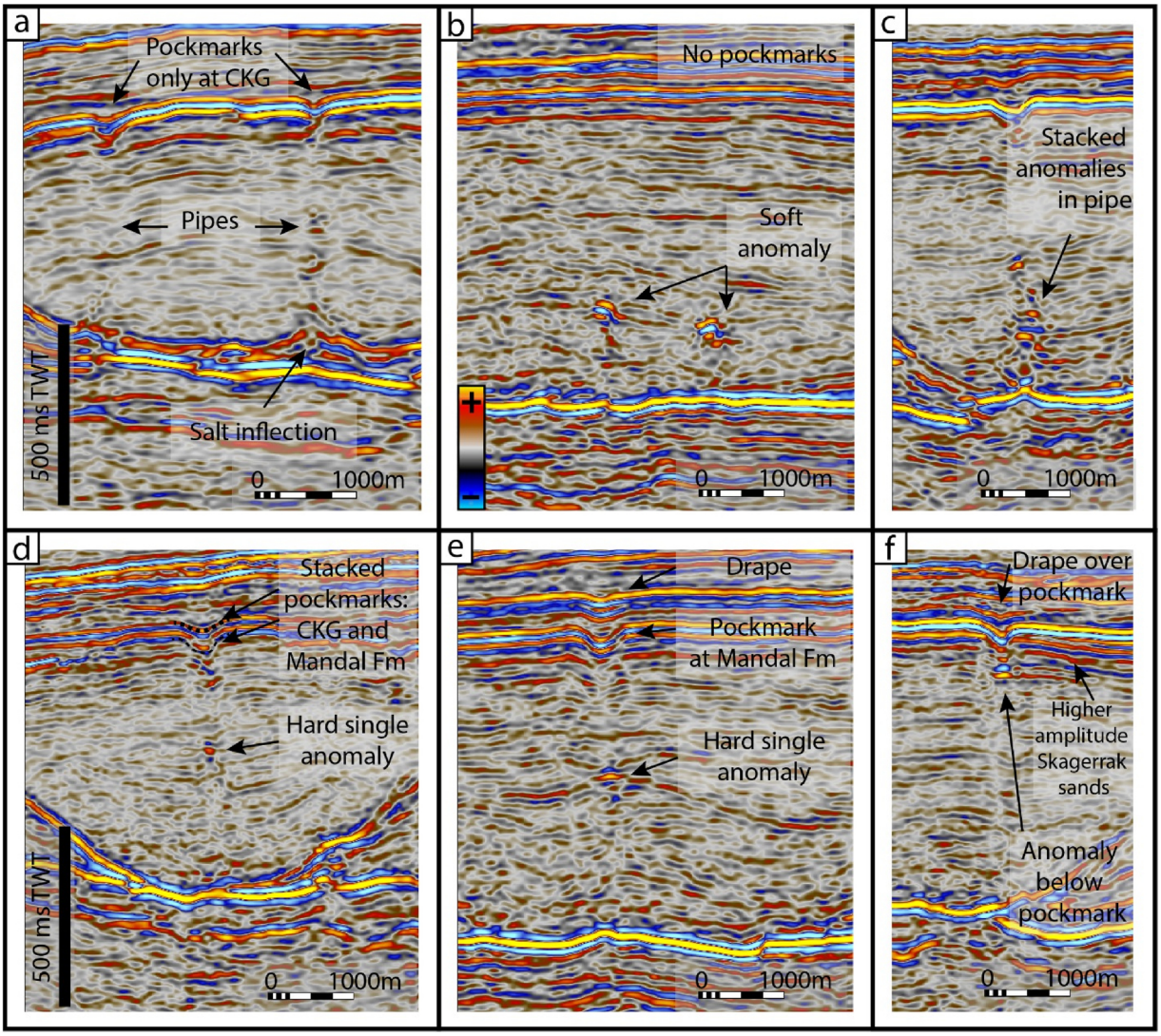

Fig. 8. Seismic examples of pipes, pockmarks and amplitude anomalies. The horizontal scale and polarity is the same across all the figures. a) Pipes terminating in pockmarks at the top of the Cromer Knoll Group, with salt inflections indicating a breach in the seal. b) Soft amplitude anomalies with no shallower pockmarks, likely comprising gas pockets. c) Stacked amplitude anomalies in a pipe. d) A single hard amplitude anomaly in a pipe, with stacked pockmarks at the Top Cromer Knoll Group and Mandal Formation horizons indicating multiple episodes of fluid flow. e) A pockmark at the Top Mandal Formation horizon, with the Cromer Knoll Group horizon 'draping' across it. f) An amplitude anomaly immediately below the pockmark and higher amplitude continuous reflections of the Skagerrak Formation.

history models and were used to interpret the timing of source rock maturation on the Jæren High. Geochemical well reports from the NPD website were investigated to summarise the hydrocarbon findings of each well.

4. Results

The results of our mapping are illustrated in Fig. 6, which highlights the key features of each interpreted horizon. Rotliegendes strata dip to the southeast and contain an array of faults that is oriented N–S and E–W. Velocity pull-ups in the basement correspond to areas of thick salt (Fig. 6a and 6b). The Upper Jurassic Mandal Formation is absent updip, towards the west, whilst the overlying Cretaceous sediments are present across the study area and shallow to the northeast. This suggests tilting of the basement and erosion or non-deposition of the Mandal Formation during the Late Jurassic, with subsequent subsidence of the Jæren High in the Cretaceous. Pockmarks are observed at the Top of the Mandal Formation, at the Top of the Cromer Knoll Group, and inside the Chalk, whilst being absent at Top Chalk level, a character suggesting that fluid venting had ended by this time (Fig. 6f). The non-uniform structure of the Top Chalk horizon implies that salt movement continued to occur until, at least, the Late Cretaceous.

The results of semi-automatic mapping and characterisation of the depressions in three surfaces – Top Mandal Formation (H3), Top Cromer Knoll Group (H4) and Intra-Chalk – as well as high-amplitude anomalies in Triassic strata, are summarised as follows.

4.1. Spatial statistics

A total of 196 depressions were identified across the three mapped surfaces, of which 18.4% occur at Intra-Chalk level, 57.7% in the Cromer Knoll Group and 24% in the Mandal Formation. Superimposing the delineated depressions onto the salt isopach map shows that depressions are solely distributed above the Triassic pods, not above the salt walls (Fig. 7). This suggests that the salt welds are tertiary migration windows, i.e. fluids have not migrated along and above the salt walls. Depressions appear to be concentrated in the centre and up-dip to the northwest of the Jæren High.

High-amplitude anomalies are found throughout the study area within the Triassic pods, immediately below depressions, and in pipes.

Table 2
Summary of the number of depressions and anomalies mapped at different seismic-stratigraphic horizons.

Horizon/ zone	No. of depressions/ anomalies	As % of mapped depressions	No. of pipes which terminate at that level	As % of total pipes	No. of anomalies in pod - of pipes that terminate at that level	As % of pipes that terminate at that level	No. of anomalies below depression	As % of depressions at that level	No. of soft anomalies
Intra Chalk	36	18.4%	0	0.0%	0	0.0%	0	0.0%	0
Cromer Knoll Group	113	57.7%	103/321	32.1%	87/103	84.5%	14/113	12.4%	0
Mandal Formation	47	24.0%	40/321	12.5%	30/40	75.0%	3/47	6.4%	0
Subtotal: depressions	196	100.0%	143	44.5%	117/143	81.8%	17/196	8.7%	0
High Amplitude Anomalies in Pods	295		178	55.5%	178	100.0%			23
Total	491		321	100.0%					23

Table 2 summarises the relationship among pipes, depressions and seismic anomalies. No amplitude anomalies were found above the depressions in the Chalk Group, revealing that gas has not migrated up to this strata and there are no gas pockets in the Chalk Group. The depth of the anomalies is variable and does not appear to correlate with any specific stratigraphic layer. Fig. 8 shows examples of the different anomalies and depressions on the seismic data. In particular, Fig. 8a shows that the Top Zechstein salt (horizon H2) was deformed (inflected up) vertically, which could be a result of fluid below the salt breaching the seal and migrating upwards with relatively high pressures.

Of the 295 mapped amplitude anomalies, 55.5% are not shown to be connected to a depression in younger strata (e.g., Fig. 8b). Discrete amplitude anomalies are prevalent in the study area (74.6%), while the remaining 25.4% are stacked in pipe columns. The majority (81.8%) of depressions have an associated high-amplitude anomaly within the pipe. All these positive (hard) anomalies indicate cemented pipes, carbonate nodules, or possibly sandstone bodies within a largely mudstone succession.

Twenty-three of the anomalies that are not associated with a depression are negative (soft) – these indicate isolated gas pockets as the presence of gas in sediments reduces the average seismic velocity of the unit, and can manifest as a negative seismic reflection if the velocity is lower than the overlying unit (Andresen et al., 2011). Of the 113 depressions observed at horizon H4 (Top Cromer Knoll Group), only 12.4% are interpreted to exhibit high-amplitude anomalies directly below the depressions. These could represent cemented zones or carbonate nodules that formed just below the surface once the pipe and depression were established. Pipes range in height from 660 m to 2280 m, with 50% of the pipes ranging between 1100 m and 1500 m (Fig. 9). Blow-out pipes of similar dimensions have been recorded offshore Nigeria (Løseth et al., 2011). The three levels of depressions mapped in this work suggest that fluid flow occurred during the Late Jurassic, Early Cretaceous and in the early Late Cretaceous, with the main episode coinciding with the end of the Early Cretaceous (top Cromer Knoll Group horizon).

4.2. Morphological analysis

Fig. 9 displays the ranges of the morphological characteristics of depressions in the form of box plots, and Table 3 summarises these plots numerically.

The Vertical Relief value describes the vertical fall from the rim of the depression to its deepest point. Vertical Relief ranges from 15 m to 178 m. The Intra-Chalk depressions have the smallest range of values, from 15 m to 71 m, with a median value of 30.5 m. These values are much smaller than those in the CKG and Mandal Formation, which have similar interquartile ranges – from 35 m to 75 m, and medians of 50 and 55 m, respectively (Fig. 9).

The width of the depressions ranges from 225 m to 842 m, with a median value of 450 m. The width of the anomalies ranges from 60 m to 575 m, with an outlier at 1170 m. The median width is 220 m, almost half of that of the depressions (Fig. 9).

Aspect ratio (width:length) is a proxy for eccentricity and ranges from 0.6 to 1.0 for all the depressions, with a median ratio of 0.88. These values reflect low eccentricity, or high sphericity. In contrast, the width:length ratios of amplitude anomalies range from 0.18 to 1.0, with a median of 0.70. This reflects the highly irregular nature of the amplitude anomalies. Due to the high sphericity of the depressions, orientation measurements are heavily biased according to the mapping algorithm function in ArcGIS, hence orientation is not deemed a reliable parameter.

Their width and vertical relief were compared for depressions coinciding vertically at different levels. The plots in Fig. 10a and c show that the width and vertical relief of depressions in the Cromer Knoll Group are always greater than those at the Intra-Chalk horizon H5, as all the points plot below the y = x line. All the Intra-Chalk depressions

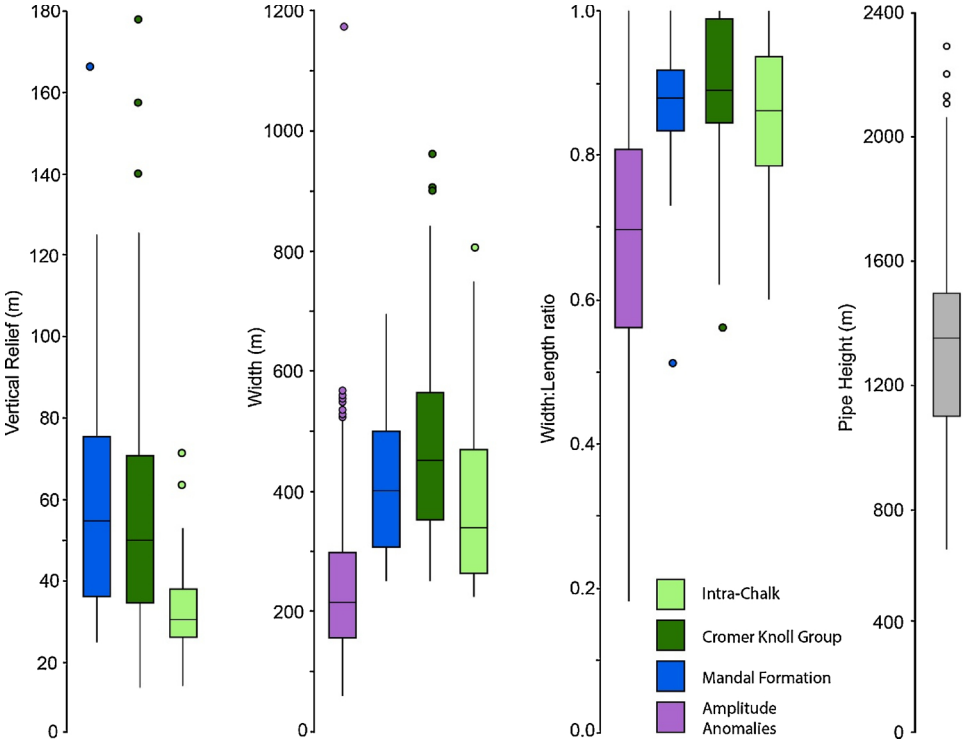

Fig. 9. Box plots summarising key morphological attributes of depressions and amplitude anomalies, from left to right: width, width:length ratio – a proxy for eccentricity, vertical relief and pipe height. Attribute ranges are consistently similar for the Mandal Formation and Cromer Knoll Group depressions, whilst those of the Intra-Chalk are generally smaller in width and vertical relief. Pipe heights vary according to the Triassic pod isopach, which increases down dip on the Jæren High.

Table 3
The minimum, maximum and median values of three morphological parameters of the depressions and amplitude anomalies: width, width:length ratio and vertical relief.

Horizon/zone	Width (m)			Width:Length ratio			Vertical Relief (m)		
	min	max	median	min	max	median	min	max	median
Intra Chalk	225	805	338	0.6	1	0.86	15	71	30.5
Cromer Knoll Group	250	842	452	0.62	1	0.89	14	178	50
Mandal Formation	250	695	401	0.73	1	0.88	25	167	55
Amplitude Anomalies in Pods	60	575	220	0.18	1	0.70	n/a	n/a	n/a

coincide with underlying depressions at horizon H4 (Top Cromer Knoll Group). The width and vertical relief are also greater for the majority of the Mandal Formation depressions when compared to depressions at the Top of the Cromer Knoll Group (Fig. 10b and d).

From these results it is interpreted that the depressions at Intra-Chalk level may not be real pockmarks, and are instead 'drape features' across the underlying pockmarks at Top Cromer Knoll Group level – the Intra-Chalk unit drapes over the underlying topography and is not formed by further fluid flow from below – and likewise for the Cromer Knoll Group depressions over the Mandal Formation pockmarks. Based on the graphs and manual investigation in Petrel, we suggest that ten depressions in the Cromer Knoll Group, overlying depressions in the Mandal Formation, are drape features, whilst the remaining seven depressions are associated with stacked pockmarks that indicate multiple episodes of fluid flow through the same pipe(s).

The total number of interpreted pipes is 321; the sum of the pipes which terminate at the Mandal Formation (12.5%), the Cromer Knoll Group (32.0%) and the anomalies without shallower depressions (55.5%). The fact that over half of the interpreted pipes are not connected to palaeo-pockmarks suggests that active seal breaching and leakage could be occurring at present across the salt welds.

4.3. Maturation models

Fig. 11 shows the burial and thermal histories from three wells: a) on the Jæren High, b) downdip from the Cod Terrace, and c) from the East Central Graben. Heat flow increased very moderately during Triassic rifting and more significantly during the growth of the North Sea Dome in the Early Jurassic, from 60 mW/m^2 up to 90 mW/m^2, decaying in the Cenozoic (Frederiksen et al., 2001). Therefore, despite the significant tectonic uplift associated with the North Sea Dome, Carboniferous coals on the Cod Terrace, and in the East Central Graben, entered the peak gas generation window as early as the Triassic and expelled gas throughout the Mesozoic. These rocks have been buried to depths over 6 km and are presently overmature (Fig. 11).

The Carboniferous on the Jæren High is 4 to 6 km deep and is interpreted to have entered the peak gas generation window during the Oligocene, remaining there to the present day. Fig. 11 shows the dramatic cooling effect of the thick salt due to its high thermal conductivity compared with clastic sediments, as the two modelled wells in a salt wall (7/7-2) and Triassic pod (7/1-1) show very different thermal histories. As heat flow has regional sources, it is likely that the thermal model from 7/7-2 is more representative of the Jæren High. However, it

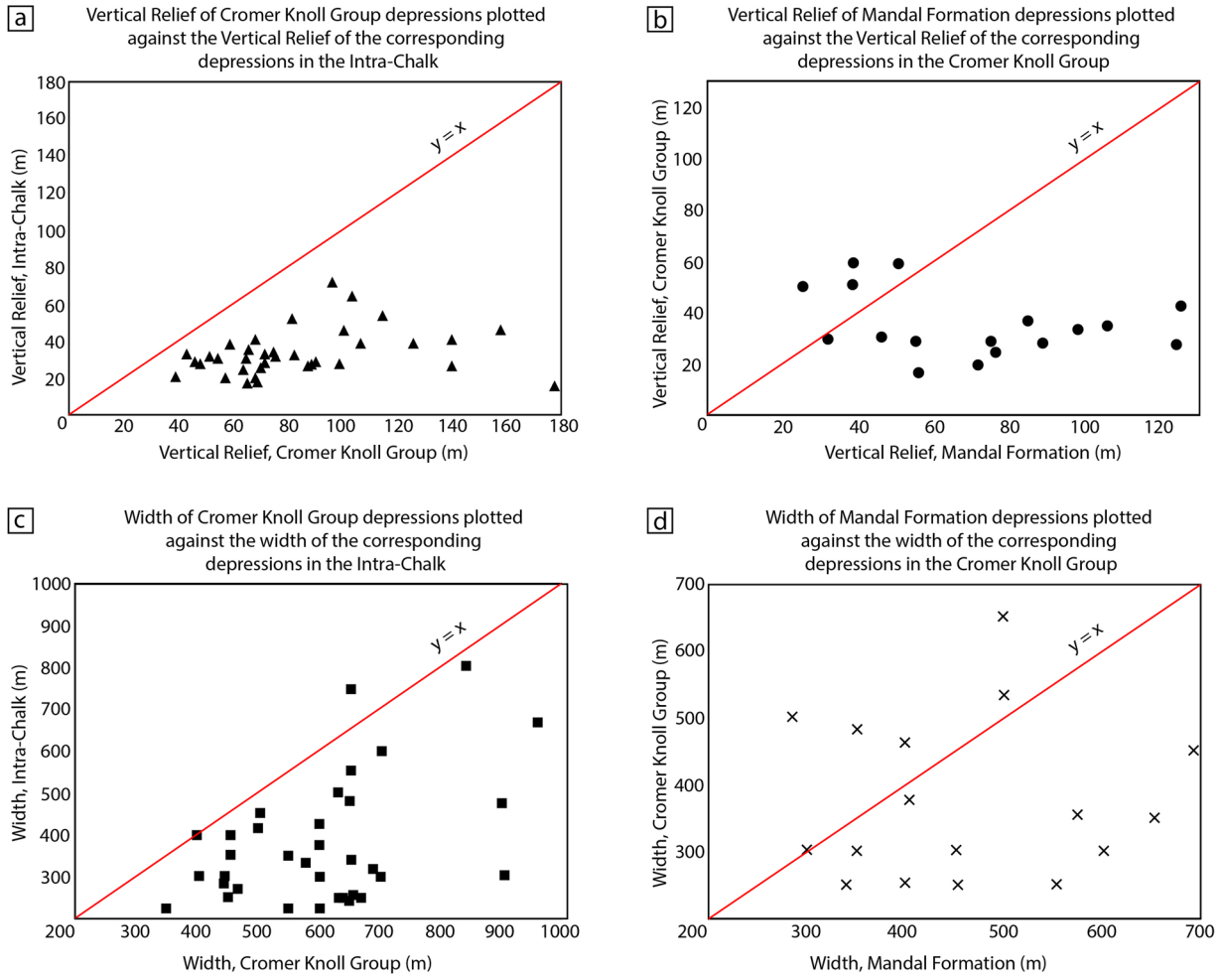

Fig. 10. Scatter Graphs comparing the Vertical Relief and Width of the Late and Early Cretaceous depressions, and Early Cretaceous and Late Jurassic depressions, for the same locations. Red lines mark y = x, where the Vertical Reliefs and Widths are equal. Graphs a) and c) show that the Vertical Relief and Width of the Cromer Knoll Group are always larger than the corresponding Intra-Chalk depressions, as the points plot below the y = x line. Graphs b) and d) show that most of the Mandal Formation depressions are larger than the corresponding Cromer Knoll Group depressions, with only five exceptions.

is also possible that some gas was generated on the Jæren High earlier in its history, possibly during Late Jurassic-Early Cretaceous rifting.

It is clear that the Upper Jurassic Mandal Formation reached the gas generation window during the Oligocene in the East Central Graben, whereas on the Cod Terrace it only reached similar conditions during the Quaternary. Whilst it could be possible for gas to migrate along the graben-bounding fault to the Jæren High in the Cenozoic, large salt diapirs extending from the basement up to the Cenozoic units line up on the graben margin, likely preventing migration across to the Jæren High. This is also proved by the presence of Paleogene sand plays above salt diapirs in this the UK waters, such as the Lomond and Pierce gas fields, sourced by gas from the Kimmeridge Clay/Mandal Formation buried in the East Central Graben. Therefore, it is unlikely that the gas forming the pipes was sourced from the Upper Jurassic Mandal Formation.

4.4. Geochemical evidence

Findings from key wells on the Jæren High are summarised in Table 4. Most of the wells drilled on the Jæren High are located above salt walls, targeting the Jurassic and Triassic sandstone units. Those that found oil were sourced from the Upper Jurassic Mandal Formation. Only three wells were drilled into the Triassic pods. The wells terminate within the upper 300 m of the Skagerrak and Smith Bank Formation, 7/1- 1, 7/4-3 and 7/7-1, all of which were dry and with no gas shows.

Well 7/1-1 was drilled adjacently to a depression in the Cromer Knoll Group, with a high-amplitude anomaly below it, but no gas shows were recorded. The maximum methane recorded was 0.37% in the top of the Upper Cretaceous Chalk, with average values remaining well below 0.1% throughout the Chalk and into the Triassic. Cores were also taken in the Chalk, which were proven to be tight. Stylolites are common, which when fractured along these lines of weakness were seen to have very thin bands of black, shale-like impurities that do not fluoresce under UV light. The Chalk Group did not contain any oil stains or visible porosity.

5. Discussion

5.1. A model for fluid migration and caprock breaching on the Jæren High

Detailed investigation of fluid flow features combined with burial history modelling allows us to describe the fluid migration history of the Jæren High, adding to the geological history described by Høiland et al. (1993). Fig. 12 summarises the history of fluid flow on the Jæren High.

Imaged pipes are shown to be rooted in the Permian Rotliegendes and cut through the Triassic succession, across salt welds. Previous studies state that salt welds formed as early as the Middle-Late Triassic due to sediment loading and salt evacuation (Høiland et al., 1993). The geometry of Triassic pods on the Jæren High supports this statement.

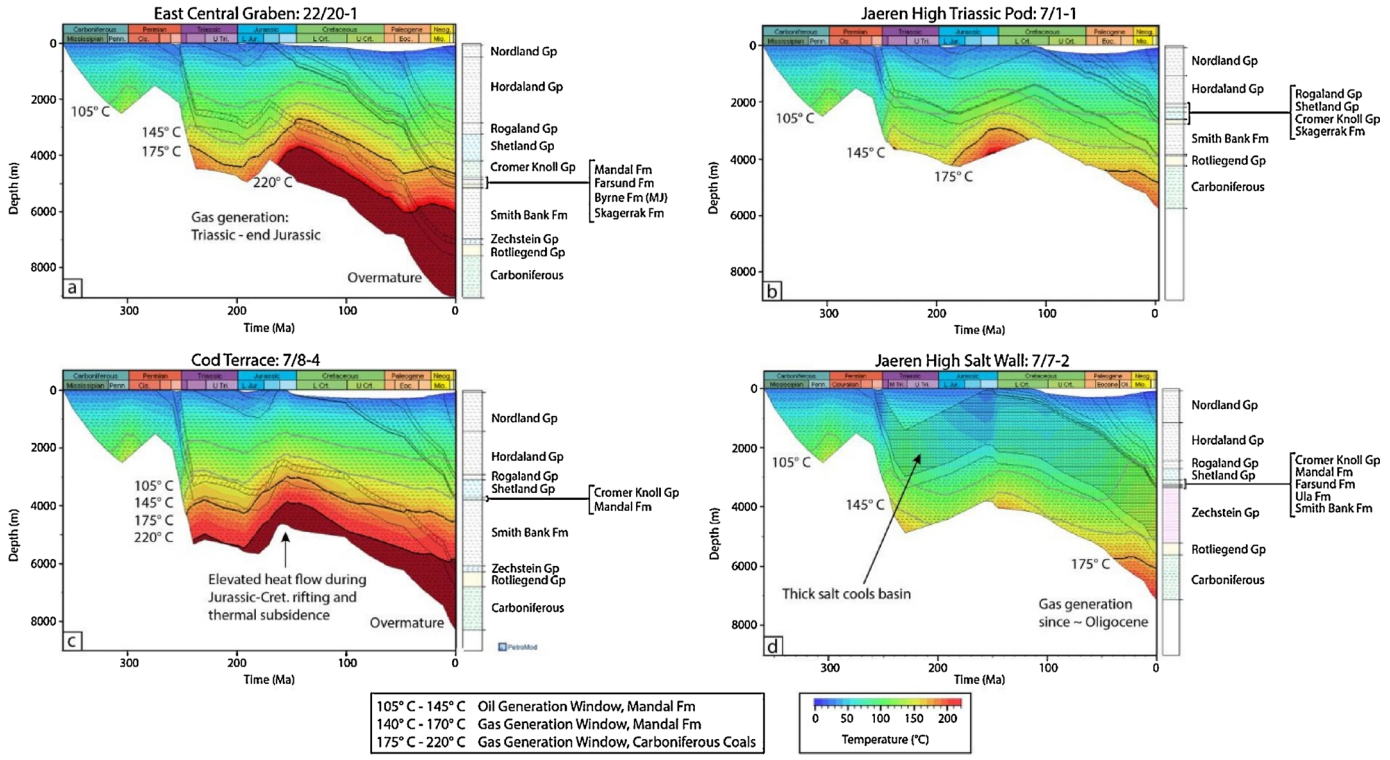

Fig. 11. Results of the burial history modelling from four wells in the Central North Sea, locations labelled in Fig. 1. The Carboniferous strata in the East Central Graben (a) and Cod Terrace (c) became gas mature for coals in the Triassic, and overmature from the Cretaceous to present. Some gas may have been produced on the Jæren High during the Late Jurassic (b), but more likely from the Oligocene to Recent, depending on the regional cooling impact of the salt. We interpret that long distance migration in the Mesozoic sourced the pipes at that time, with local maturation and migration occurring at present.

Seismic reflections in the Smith Bank Formation bend down onto the Rotliegend Group and salt wall edges, forming turtle anticlines, a character indicating grounding of sediment pods (e.g. Karlo et al., 2014), whilst the younger Triassic reflections level out and become parallel towards the top of the pods (Fig. 12). A salt weld cannot be formed solely by salt evacuation, as the boundary drag forces increase as salt thickness decreases (Jackson and Cramez, 1989; Hudec and Jackson, 2007). The remaining salt can be removed by dissolution (Wagner and Jackson, 2011).

Pipes terminate in the form of depressions within the Mandal Formation (Late Jurassic) and Cromer Knoll Group (Early Cretaceous), and are interpreted to form pockmarks at this level. The build-up of excessive gas and fluid within the Rotliegend Group caused high overpressures to develop. Once the capillary entry pressure of the overlying seal was exceeded, gas and fluid migrated across salt welds and through the Triassic mudstone succession by a hydrofracturing mechanism, forming pipes that terminated at the palaeo-seafloor as those described in Moss and Cartwright (2010). Sediment was removed into the water column, leaving behind a depression known as a pockmark. Therefore, the timing of tertiary fluid migration is indicated by the level of the pockmark; the pipes terminating in pockmarks formed during the Late Jurassic-Early Cretaceous. The migration of gas could have occurred over years to centuries or more (Cathles et al., 2010). The term ‘craters’ may be a more apt name for these features, owing to their large sizes, as modern, recorded pockmarks are typically up to 300 m wide and range in vertical relief between 1 m and 80 m deep (Hovland and Judd, 1988; Gay et al., 2006). Large pockmarks have nonetheless been described on the Scotian Shelf as typically measuring 10–700 m in diameter and being 1–45 m deep (Hovland et al., 2002).

It is possible for pipes to form due to rapid compaction and dewatering of mudstones (Berndt et al., 2003). However, the pipes identified on the Jæren High are rooted in Rotliegendes strata and, in most cases, generate local folds (inflections) within the salt (Fig. 8). This indicates a breach in the seal and fluid bypass through the salt welds, supporting the interpretation of gas and fluid expulsion from depth. This interpretation also relates to giant pockmarks found at the top of Lower Cretaceous Marl in the Lower Saxony Basin of the Netherlands (Strozyk et al., 2018). F. Strozyk and co-authors interpreted that gas sourced from Carboniferous coals migrated across salt welds into shallower Cretaceous strata, forming giant pockmarks.

Results show that 28% of the pipes with depressions formed during the Late Jurassic, whilst the main period of fluid flow on the Jæren High occurred during the Early Cretaceous, as 72% of the pockmarks terminate at this level. The pipes forming stacked pockmarks may have been active throughout this time, whilst those generating discrete pockmarks were plugged and cemented at an early stage (e.g. Hovland et al., 2005; Andresen et al., 2011). Thirty-six depressions were mapped at the Intra-Chalk level. However, morphological analysis shows that the Intra-Chalk depressions are always associated with corresponding depressions at the Top Cromer Knoll Group horizon H4, which are consistently greater in width and vertical relief. This lead us to interpret the depressions at Intra-Chalk level as drape features due to differential compaction. Still, it is possible that low-level seepage occurred after the initial formation of the pockmarks. Not all the depressions show these ‘drape’ features, perhaps due to laterally varying lithology in the overlying Chalk Group, or due to thickness variations and different degrees of differential compaction.

Although the pipes are interpreted to be sourced from Rotliegendes strata, the gas is likely to have been expelled from deeper (Carboniferous) coals. The burial history plot for the Jæren High shows that Carboniferous strata did not reach sufficiently high temperatures to enter the gas maturation window during the Mesozoic (Fig. 11a). However, investigation of nearby potential source kitchens showed that the Carboniferous entered the gas maturation window during the Triassic, remaining there throughout the Mesozoic (Fig. 11b and c). We interpret that gas could have been sourced to the west of the Jæren

Table 4
Summary of the objectives, drilling location with respect to salt walls or Triassic pods, and results of the key wells on the Jæren High. Data has been summarised from the Norwegian Petroleum Directorate web pages.

Well	Objective(s)	Salt Wall or Triassic Pod; Formation TD	Findings
6/3-1 Gaupe Field	Primary – Jurassic and Triassic sandstones; Secondary – Paleocene sandstones and Upper Cretaceous porous/fractured chalk	Salt Wall; TD Skagerrak Fm.	72 m oil and gas condensate column discovered within Jurassic and Triassic reservoirs. Paleocene sandstones absent. Logs suggested hydrocarbons in the Chalk, but flow tests were negative; proved a tight formation.
6/3-2	Primary – Jurassic and Triassic sandstones; Secondary – Cretaceous chalk and Rotliegendes sandstones	Salt Wall; TD Rotliegend Gp.	Oil shows, but no moveable hydrocarbons within the Chalk, Ula or Skagerrak sands. Poor reservoir quality in the Chalk, < 0.02 mD permeability. Rotliegendes strata were water saturated without trace of hydrocarbons.
7/3-1	All horizons down to Permian Rotliegendes	Salt Wall; TD Carboniferous	Triassic and Lower Jurassic units missing. No spores – for maturity assessment – observed in samples of Rotliegendes and Carboniferous. 8 m of Carboniferous drilled, no hydrocarbon source potential. Dry well.
7/1-1	Triassic Skagerrak Fm.	Triassic Pod; TD 147 m into Skagerrak Fm.	Jurassic units absent. Dry well.
7/4-1	Upper Jurassic sandstones	Salt Wall; TD Zechstein Gp.	17 m Ula Fm. penetrated, no hydrocarbons. Triassic-Middle Jurassic absent. Dry well.
7/4-3	Primary – Triassic Skagerrak Fm. Secondary – Upper Cretaceous-Paleocene Ekofisk and Tor Fms.	Triassic Pod; TD 267 m into Smith Bank Fm.	No Skagerrak sandstones, only Smith Bank floodplain mudstones. Jurassic absent. Dry well.
7/7-2 Brynhild Field	Upper Jurassic sandstones	Salt Wall; TD Zechstein Gp.	19.5 m oil column discovered within the Ula Fm. Sandstones. No gas cap. 40 m of Smith Bank Fm. present. Good oil shows in Mandal Fm. – excellent oil prone source rock and oil window maturity.
7/4-2 Brynhild Field	Primary – appraise well 7/7-2. Secondary – Triassic Smith Bank Fm.	Salt Wall; TD Zechstein Gp.	Shows in Ula Fm. and 4 m of Skagerrak Fm. No shows in underlying Triassic – Skagerrak and Smith Bank Fm. present.
7/7-1	Primary – Triassic sandstones Secondary – Paleocene sandstones	Triassic Pod; TD 212 m into Smith Bank Fm.	Paleocene sandstones pinch out in blocks 7/4 and 7/7. No Skagerrak Fm. Dry well.
23/11-3	Upper Jurassic sandstones	Salt Wall; TD Smith Bank Fm.	Oil shows. No Skagerrak Fm. Abandoned as a dry well.

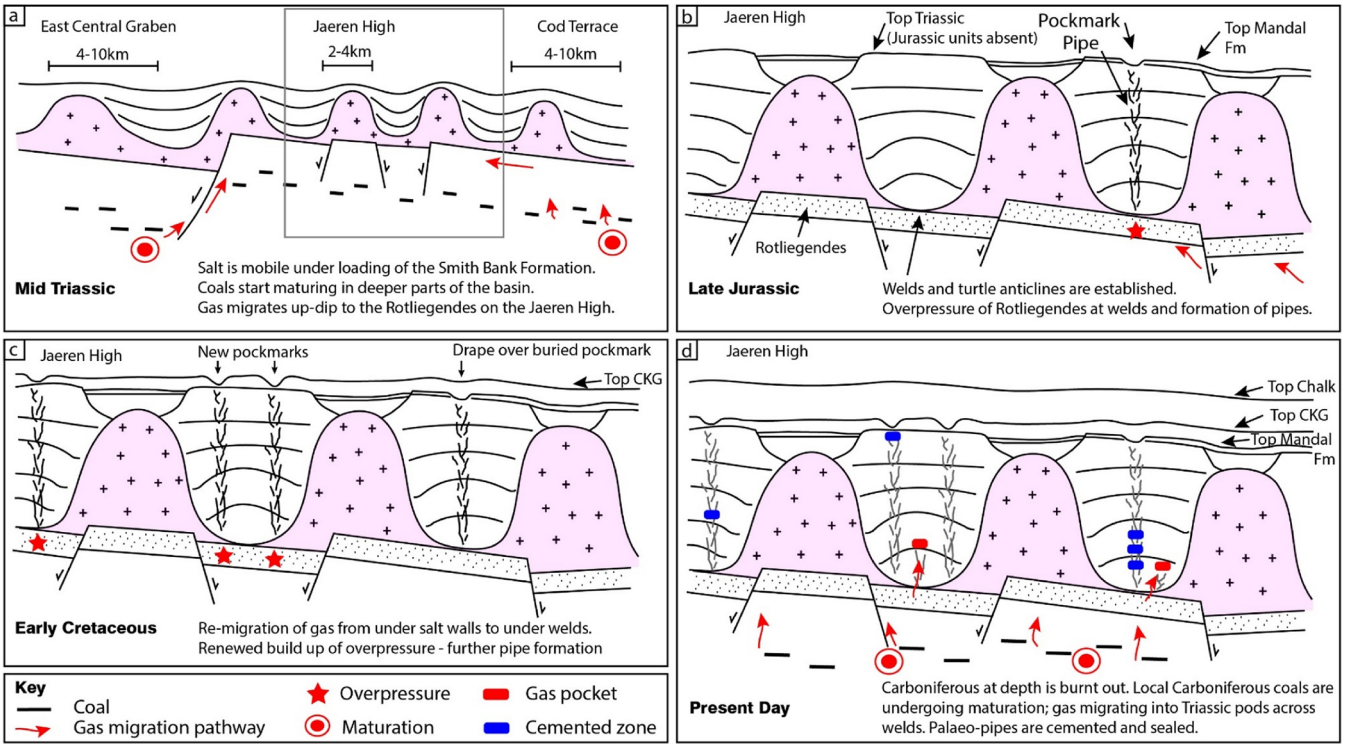

Fig. 12. Summary of the fluid migration evolution of the Jæren High, from a) to d). a) Shows a regional schematic, modified from Hodgson et al. (1992). b) To d) focus on the Jæren High only, marked in a grey box in a). Gas pockets (red) and cemented zones (blue) are interpreted from 'soft' and 'hard' anomalies respectively. Arrows indicate migration pathways. CGK – Cromer Knoll Group.

High in the East Central Graben, migrating vertically along the graben-bounding fault. Importantly, the presence of pipes and pockmarks up to 40 km away from this fault, down-dip of the Jæren High, suggests that large volumes of gas accumulated there and putatively sourced gas to the study area from the southeast, i.e. from the Cod Terrace region in Norwegian waters. These two source kitchens, exceeding 6 km depth, are presently overmature.

5.2. Data limitations and the importance of understanding leakage risk

Morphological analyses have been undertaken to describe the pockmarks and discern their formation mechanisms. However, it became apparent that due to the resolution of the data and the scale of variation of the morphological characteristics, only a few basic parameters were viable for analysis, e.g. width, vertical relief and eccentricity. Small-scale changes in slope and roughness may give insight into whether the depressions are pockmarks, sinkholes or hypogenic collapse structures, but these variations are not resolved on the interpreted seismic volume. However, as the depressions are situated within the marine shales of the Mandal Formation, and marls of the Cromer Knoll Group, it is not possible for the depressions to be hypogenic karst structures. Furthermore, compaction and burial will have removed or distorted morphological features that would be clear at the seabed or shallow subsurface. This could impact interpretations as the depressions within the Chalk Group, considered to be 'drape' features, can actually represent active fluid flow, but are smaller due to the differing lithology of the Chalk Group compared to the Cromer Knoll Group and Mandal Formation.

Xia and Wilkinson (2017) summarised the geological reasons for exploration failure in boreholes drilled on the UK Continental Shelf. They noted that 6% of the wells failed due to poor caprock sealing, 6% due to incorrect trap depth prediction, and 21% due to incorrect prediction of trap geometry and extent. This emphasizes the importance of analysing fluid migration and leakage across broad regions of sedimentary basins.

We interpret the 'hard' anomalies in this work to be cemented zones or carbonate concretions. Only 13% of the anomalies that are not connected to pockmarks are 'soft' – if these represent pockets of gas, then it is possible that leakage is occurring at present, an unfavourable setting when assessing sites for CO_2 injection. Fluid flow conduits are actively bypassing salt welds and the overlying mudstone successions, despite thicknesses of up to ~2200 m. Thickness is one of the four seal risk factors described by Downey (1984) together with capillary entry pressures, lateral lithological variations and variable degrees of fracturing. A thicker seal unit is considered to be more effective, but is still dependent on the height of the fluid column and resulting build-up of pore-pressure. On the Jæren High, with seal thickness ranging from 650 to 2200 m, the seal was still breached (Fig. 8).

In summary, the method presented here is important for predicting the mechanisms behind pipe formation and whether gas can be trapped in the pipe itself. It also helps discerning if the pipes are active and gas is migrating towards a shallower reservoir, or even leaking towards the surface. If depressions had been mainly found within the Chalk Group, then these could be collapse structures formed due to hypogenic fluid migration when the Chalk Group was buried, as opposed to fluids venting onto the sea floor (Masoumi et al., 2014). This also means that fluid migration could have happened relatively recently in time, and gas should be trapped within the Chalk Group. However, the depressions are found within the marls and shales, rebuking such an interpretation. Exploration wells consistently found tight limestones with very low gas concentrations in the Chalk Group, so it is unlikely that gas has accumulated at this level, and that the pipes are active at present.

6. Conclusions

This study shows how a novel integrated method using GIS, borehole geochemical and 3D seismic data can be used to better visualise and model fluid flow features that have previously been overlooked, or

unresolved. Understanding the timing of tertiary fluid migration and the locations of fluid flow pathways is important for assessing and managing the risk of fluid escape for both hydrocarbon exploration and carbon capture and storage. The results of this work can be summarised as follows:

a) In the study area, large vertical fluid pipes sourced in the Permian Rotliegend Group cut across 600 to 2300 m of Triassic mudstones, across salt minibasins, or pods. These pipes terminate as pockmarks in the Upper Jurassic Mandal Formation and Lower Cretaceous Cromer Knoll Group. This indicates the timeframe of vertically focused fluid expulsion and the potential for fluids to leak from these established conduits.
b) As the pockmarks range from 200 to 800 m in width and 15 to 200 m in vertical extent, they reflect the transport of extremely large volumes of fluid, which were required to form features of this scale. The gas migrated into the Mesozoic strata sequence sourced from the East Central Graben to the west, and Cod Terrace to the southeast.
c) Long-distance vertical and up-dip migration occurred towards the Jæren High, until pore-fluid pressures were sufficiently high to breach the Smith Bank Mudstone Formation seal.
d) Thus, high-amplitude anomalies represent both cemented pipes and potential gas pockets, whose presence indicates increased risk as a potential flow pathway. These are crucial data to determining where active leakage is occurring at present, and whether a site will be suitable for containment and geological storage of carbon dioxide.

Declarations of interest

None.

Acknowledgements

The work in this study was conducted during a PhD study undertaken as part of the Natural Environment Research Council (NERC) Centre for Doctoral Training (CDT) in Oil and Gas. It is sponsored by Cardiff University and the British Geological Survey (BGS) via the British University Funding Initiative (BUFI) grant number GA/16S/007, whose support is gratefully acknowledged. The British Geological Survey (BGS) is thanked for provision of the BGS Seabed Mapping Toolbox, as well as Maxine C. Akhurst from the BGS for aiding to proof read. We thank the BGS and Norwegian Petroleum Directorate (NPD) for access to well data. We also acknowledge the Department of Geoscience and Petroleum, Norwegian University of Science and Technology (NUST) for access to 2D seismic data and Norwegian well logs. We thank PGS for access and permission to publish examples from their 3D seismic data volumes. We also acknowledge Schlumberger (for Petrel® and Petromod®) and ESRI (for ArcGIS) for providing academic licences to Cardiff's 3D Seismic Lab. We also thank IJGGC editor Neil Wildgust, Simon Müller and an anonymous reviewer for their constructive comments.

Appendix A. Seismic Stratigraphy

Carboniferous/Devonian units

Pre-salt units are poorly resolved, consisting of mostly chaotic seismic reflections. Some continuous reflections and faults are clear on seismic data. The units dip to the southeast, pinching out towards the crest of the high to the northwest.

Horizon 1 - Top Rotliegend Group (Late Permian)

The top of the Rotliegend Group is marked by a bright hard seismic reflection below which sub-parallel, continuous reflections are observed. No wells penetrate the Carboniferous, so it is unclear as to the true depth extent of the Rotliegend Group. The Rotliegend Group is cross-cut by faults trending NNW to E.

Small 'ridges' are seen in map view on the surface of the Rotliegend Group within the salt weld zones, which may be an imaging artefact, or a consequence of disruption due to fluid flow related to overlying pipes. The Rotliegend Group was coupled with the top of the basement during the main rifting episode and is tilted to the SE.

Horizon 2 – Top Zechstein Group (latest Permian)

The top of the Zechstein Group is marked by a bright 'hard' seismic reflection. Where the contact is near vertical, imaging is poor and the contact is inferred. The Zechstein Group is preferentially located on relative basement highs, and form salt walls with a predominant N–S trend and minor E–W trend, with intervening salt welds (Fig. 6b – salt isopach). The thickness of the Zechstein Group was calculated using an interval velocity of 4650 m/s from well 6/3-2, and is shown to vary from 0 m to ~2300 m, thickening southeastwards.

The interior of some salt walls consists of poorly imaged, low amplitude, chaotic, discontinuous seismic reflections. In contrast, more extensive salt walls contain continuous, horizontal reflections, similar to the overlying clastic units, and could be mistaken as such. However, well calibration confirms the presence of the Zechstein Group.

Smith Bank – Skagerrak Formation (Triassic)

The Triassic units are found in large pods between salt walls. Seismic reflections are of low amplitude due to the homogeneity of predominantly silt and claystones. Where the Triassic strata are well imaged, a combination of diverging and parallel internal reflections is observed, with onlap both within the pods and onto the adjacent salt walls. Downlap onto the Rotliegend Group is common where turtle-back anticlines have formed, indicating grounding of sediment pods and salt weld formation as early as the Triassic. Thin Triassic units have been identified above some salt walls in wells 6/3-2 (145 m) and 7/7-2 (45 m), but may not be present everywhere. Narrow, chaotic pipes cross cut the Triassic pods, but are poorly imaged due to the semi-transparent nature of the Triassic strata, apart from occasional amplitude anomalies. The top Triassic does not show a clear seismic reflection and it was not interpreted.

Horizon 3 – Top Mandal Formation (Late Jurassic)

Lower-Middle Jurassic strata are assumed to be absent across the Jæren High as they have not been crossed by any wells – the area was emergent

during the Early Jurassic doming of the North Sea. Upper Jurassic strata have a limited distribution, being absent above most of the Triassic pods and present directly above salt walls – the thickest section encountered is 157 m in well 6/3-2.

The Mandal Formation manifests as a high-amplitude seismic reflection that is characteristic of a 'hot shale', just as the Kimmeridge Clay Formation, its UK equivalent. The Mandal Formation is also clearly marked by a sharp peak in gamma ray curves (Fig. 4). Towards the east of the study area, where the Mandal Formation is interpreted to occur above the Triassic pods, some depressions are seen, with pipes imaged below (Fig. 6c).

Horizon 4 – Top Cromer Knoll Group (Early Cretaceous)

The Base Cretaceous Unconformity lies across the Triassic pods and Upper Jurassic strata above salt walls. The Top Cromer Knoll Group is also an unconformity representing the top of either the Rødby, Sola, Tuxen or the Åsgard Formations. The Cromer Knoll Group comprises continuous, gently undulating internal seismic reflections. The top of this Group marks the transition from marls to the Chalk Group, and manifests as a bright hard seismic reflection, draping the full extent of the Triassic-Jurassic pods-interpods. This surface is shown to be covered in large circular depressions (Fig. 6d).

Horizon 5 - Intra-Chalk Group (Late Cretaceous)

This horizon is an intra-Chalk unconformity, possibly corresponding to the Top Hod Formation. It varies greatly in amplitude, but is largely continuous, draping the underlying topography. In some cases, the surface contains depressions above those seen in the Cromer Knoll Group.

Horizon 6 - Top Chalk Group (Late Cretaceous – Early Paleocene)

The Top Chalk is another bright, continuous seismic reflection, marking the transition from Cretaceous-Paleocene Chalk to Tertiary clastics. Internal seismic reflections in the Chalk Group are generally parallel to sub-parallel and of low amplitude. Some faults appear to cut the Chalk Group, whilst no depressions are interpreted inside this unit.

Top Sele Formation (Paleocene)

The Paleocene unit contains mostly low amplitude, parallel to sub-parallel internal reflections representing hemipelagic mudstones onlapping onto basin highs. The Sele Formation is cut by high-angle, high-density polygonal faults that extend into younger strata.

Hordaland and Nordland Groups (Paleocene – Recent)

The Hordaland and Nordland Groups, from Eocene to present, consist of parallel, continuous reflections, with occasional, weakly sub-parallel and onlapping seismic reflections demonstrating the largely hemipelagic nature of their strata.

Appendix B. Maturation Model Parameters

Palaeo-water depth values were estimated based on: a) the typical water depths for the lithologies encountered in wells, b) geological well reports from the Norwegian Petroleum Directorate, and c) data in Frederiksen et al. (2001) and Haq et al. (1988). The sea water temperature was calculated by an algorithm embedded in Petromod®, which takes into account palaeo-water depth and latitude through time. Heat flow (thermal history) was also obtained from Frederiksen et al. (2001).

Age (Ma)	Palaeo-Water Depth (m)	Seawater Temperature (°C)	Heat Flow (mW/m^2)
0	82	5.0	55
5	100	5.8	56
12	120	8.8	57
20	180	15.6	58
25	200	17.0	58
30	250	16.0	59
40	280	16.2	60
60	300	17.3	62
64	300	13.4	63
70	287	17.7	64
88	227	20.8	67
102	160	22.2	68
106	78	23.3	69
113	21	24.3	76
122	0	n/a	80
138	0	n/a	86
157	0	n/a	89
161	0	n/a	76
170	0	n/a	72
174	0	n/a	70
177	0	n/a	67
180	19	18.3	67
184	34	18.7	65
187	52	17.8	65
190	74	17.8	62

194	71	17.9	61
195	63	18.0	61
197	34	19.0	60
200	0	n/a	60
250	0	n/a	69
252	32	24.2	64
255	50	24.0	60
260	28	23.3	59
262	0	23.7	59
280	0	n/a	65
290	0	n/a	75
295	0	n/a	81
305	0	n/a	72
310	0	n/a	65
320	0	n/a	60
333	0	n/a	58
359	0	n/a	58

References

Agada, S., Jackson, S., Kolster, C., Dowell, N.Mac, Williams, G., Vosper, H., Krevor, S., 2017. The impact of energy systems demands on pressure limited CO2storage in the Bunter Sandstone of the UK Southern North Sea. Int. J. Greenh. Gas Control. 65 (August), 128–136. https://doi.org/10.1016/j.ijggc.2017.08.014.

Ahmadi, Z.M., Sawyers, M., Kenyon-Roberts, S., Stanworth, C.W., Kugler, K.A., Kristensen, J., Fugelli, E.M., 2003. Paleocene. In: Evans, D., Graham, C., Armour, A., Bathurst, P. (Eds.), The Millennium Atlas: Petroleum Geology of the Central and Northern North Sea. The Geological Society of London, London, pp. 235–259.

Alves, T.M., Elliott, C., 2014. Fluid flow during early compartmentalisation of rafts: A North Sea analogue for divergent continental margins. Tectonophysics 634, 91–96. https://doi.org/10.1016/j.tecto.2014.07.015.

Andresen, K.J., Huuse, M., Schødt, N.H., Clausen, L.F., Seidler, L., 2011. Hydrocarbon plumbing systems of salt minibasins offshore Angola revealed by three-dimensional seismic analysis. Bull. 95 (6), 1039–1065. https://doi.org/10.1306/12131010046.

Arts, R.J., Vandeweijer, V.P., Hofstee, C., Pluymaekers, M.P.D., Loeve, D., Kopp, A., Plug, W.J., 2012. The feasibility of CO2 storage in the depleted P18-4 gas field offshore the Netherlands (the ROAD project). Int. J. Greenh. Gas Control. 11 (SUPPL), 10–20. https://doi.org/10.1016/j.ijggc.2012.09.010.

Badley, M.E., 1985. Practical Seismic Interpretation. IHRDC Press, Boston, MA: United States.

Berndt, C., Bünz, S., Mienert, J., 2003. Polygonal fault systems on the mid- Norwegian margin: a long-term source for fluid flow. Subsurface Sediment Mobilisation, Geological Society 216. Special Publications, London, pp. 283–290. https://doi.org/10.1144/GSL.SP.2003.216.01.18. 1.

Brown, A.R., 2011. Interpretation of Three-Deimensional Seismic Data. Society of Exploration Geophysicists and American Association of Petroleum Geologists.

Cartwright, J., Huuse, M., Aplin, A., 2007. Seal bypass systems. Bull. 91 (8), 1141–1166. https://doi.org/10.1306/04090705181.

Cartwright, J., Santamarina, C., 2015. Seismic characteristics of fluid escape pipes in sedimentary basins: Implications for pipe genesis. Mar. Pet. Geol. https://doi.org/10.1016/j.marpetgeo.2015.03.023.

Cathles, L.M., Su, Z., Chen, D., 2010. The physics of gas chimney and pockmark formation, with implications for assessment of seafloor hazards and gas sequestration. Mar. Pet. Geol. 27 (1), 82–91. https://doi.org/10.1016/j.marpetgeo.2009.09.010.

Clark, J.A., Cartwright, J.A., Stewart, S.A., 1999. Mesozoic dissolution tectonics on the West Central Shelf, UK Central North Sea. Mar. Pet. Geol. 16 (3), 283–300. https://doi.org/10.1016/S0264- (98)00040.

Copestake, P., Sims, A. P., Crittenden, S., Hamar, G. P., Ineson, J. R., Rose, P. T., & Tringham, M. E. (2003). Lower Cretaceous. In In: The Millennium Atlas: petroleum geology of the Central and Northern North Sea. Evans, D, Graham, C, Armour, A, and Bathurst, P (London: The Geological Society of London). (pp. 191– 211).

Crow, W., Brian Williams, D., William Carey, J., Celia, M., Gasda, S., 2009. Wellbore integrity analysis of a natural CO2 producer. Energy Procedia 1 (1), 3561–3569. https://doi.org/10.1016/j.egypro.2009.02.150.

de Mahiques, M. M., Schattner, U., Lazar, M., Sumida, P. Y. G., & Souza, L.A.P. de. (2017). An extensive pockmark field on the upper Atlantic margin of Southeast Brazil: spatial analysis and its relationship with salt diapirism. Heliyon, (e00257), 1–21. https://doi.org/10.1016/j.heliyon.2017.e00257.

Downey, M.W., 1984. Evaluating Seals for Hydrocarbon Accumulations. American Association of Petroleum Geologists Bulletin 68 (11), 1752–1763. https://doi.org/10.1306/AD461994-16F7- 11D7-8645000102C1865D.

Eiken, O., Ringrose, P., Hermanrud, C., Nazarian, B., Torp, T.A., Høier, L., 2011. Lessons Learned from 14 years of CCS Operations: Sleipner, In Salah and Snohvit. Energy Procedia 4, 5541–5548. https://doi.org/10.1016/j.egypro.2011.02.541.

Erratt, D., Thomas, G., Wall, G.R., 1999. The evolution of the Central North Sea rift. Petroleum Geology of Northwest Europe: Proceedings of the 5th Conference on Petroleum Geology of NW. Europe, at the Barbican Centre 63–82.

Fraser, S.I., Robinson, A.M., Johnson, H.D., Underhill, J.R., Kadolsky, D.G.A., Connell, R., Ravnås, R., 2002. Upper jurassic. In: Evans, D., Graham, C., Armour, A., Bathurst, P. (Eds.), The Millennium Atlas: Petroleum Geology of the Central and Northern North Sea. The Geological Society of London, London, pp. 157–189.

Frederiksen, S., Nielsen, S.B., Balling, N., 2001. Post-Permian evolution of the Central North Sea: A numerical model. Tectonophysics 343 (3–4), 185–203. https://doi.org/10.1016/S0040- 1951(01)00224-4.

Gafeira, J., Long, D., Diaz-Doce, D., 2012. Semi-automated characterisation of seabed pockmarks in the Central North Sea. Near Surf. Geophys. 10 (4), 303–314.

Gafeira, J., Dolan, M., Monteys, X., 2018. Geomorphometric Characterization of Pockmarks by Using a GIS-Based Semi-Automated Toolbox. Geosciences 8 (5), 154. https://doi.org/10.3390/geosciences8050154.

Gay, A., Lopez, M., Cochonat, P., Séranne, M., Levaché, D., Sermondadaz, G., 2006. Isolated seafloor pockmarks linked to BSRs, fluid chimneys, polygonal faults and stacked Oligocene-Miocene turbiditic palaeochannels in the Lower Congo Basin. Mar. Geol. https://doi.org/10.1016/j.margeo.2005.09.018.

Geldof, J.-B., Gafeira, J., Contet, J., Marquet, S., 2014. GIS analysis of pockmarks from 3D seismic exploration surveys. Offshore Technology Conference 25088, 1–10.

Glennie, K., Underhill, J., 1998. Origin, Development and Evolution of Structural Styles. Petroleum Geology of the North Sea: Basic Concepts and Recent Advances. https://doi.org/10.1002/9781444313413.ch2.

Glennie, K.W., 1998. Lower Permian - Rotliegend. In Petroleum Geology of the North Sea: Basic Concepts and Recent Advances, fourth edition. pp. 137–173. https://doi.org/10.1002/9781444313413. ch5.

Goldsmith, P.J., Hudson, G., Van Veen, P., 2003. Goldsmith Et al., 2003.pDf.Goldsmith Et al., 2003.pDf.

Guen, Y., Le, Huot, M., Loizzo, M., Poupard, O., 2011. Well integrity risk assessment of Ketzin injection well (Ktzi-201) over a prolonged sequestration period. Energy Procedia 4, 4076–4083. https://doi.org/10.1016/j.egypro.2011.02.350.

Haq, B.U., Hardenbol, J., Vail, P.R., 1988. Mesozoic and Cenozoic Chronostratigraphy and Eustatic Cycles 42. SEPM Special Publication, pp. 71–108. https://doi.org/10.2110/pec.88.01.0071.

Hodgson, N.A., Farnsworth, J., Fraser, A.J., 1992. Salt-related tectonics, sedimentation and hydrocarbon plays in the Central Graben, North Sea, UKCS. Geol. Soc. London Spec. Publ. 67 (1), 31–63. https://doi.org/10.1144/GSL.SP.1992.067.01.03.

Høiland, O., Kristensen, J., Monsen, T., 1993. Mesozoic evolution of the jaeren High area, Norwegian Central North Sea. Petroleum Geology of Northwest Europe: Proceedings of the 4th Conference on Petroleum Geology of NW. Europe, at the Barbican Centre, London 1189–1195. https://doi.org/10.1144/0041189.

Hovland, M., Gardner, J.V., Judd, A.G., 2002. The significance of pockmarks to understanding fluid flow processes and geohazards. Geofluids 2 (2), 127–136. https://doi.org/10.1046/j.1468- 8123.2002.00028.x.

Hovland, M., Judd, a.G., 1988. Seabed Pockmarks and Seepages — Impact on Geology, Biology and the Marine Environment. Graham & Trotman Ltd., London. https://doi.org/10.1016/0264- 8172(89)90010-X.

Hovland, M., Svensen, H., Forsberg, C.F., Johansen, H., Fichler, C., Fosså, J.H., Jonsson, R., Rueslåtten, H., 2005. Complex pockmarks with carbonate-ridges off mid-Norway: Products of sediment degassing. Mar. Geol. 218 (1–4), 191–206. https://doi.org/10.1016/j.margeo.2005.04.005.

Hudec, M.R., Jackson, M.P.A., 2007. Terra Infirma: Understanding salt tectonics. Earth-Science Reviews 82 (1–2), 1–28. https://doi.org/10.1016/j.earscirev.2007.01.001.

Jackson, M.P.A., Cramez, C., 1989. Seismic recognition of salt welds in salt tectonics regimes. SEPM Gulf Coast Section Tenth Annual Research Conference Program and Abstracts. pp. 66–71.

Karlo, J.F., Buchem, F.S.P., Van, Moen, J., Milroy, K., 2014. Salt tectonics and interpretation Triassic-age salt tectonics of the Central North Sea. Interpretation 2 (4), 19–28.

King, L.H., MacLean, B., 1970. Pockmarks on the Scotian shelf. Bulletin of the Geological Society of America.

Li, B., Zhou, F., Li, H., Duguid, A., Que, L., Xue, Y., Tan, Y., 2018. Prediction of CO 2 leakage risk for wells in carbon sequestration fields with an optimal artificial neural network. Int. J. Greenh. Gas Control. 68 (18), 276–286. https://doi.org/10.1016/j.ijggc.2017.11.004.

Løseth, H., Gading, M., Wensaas, L., 2009. Hydrocarbon leakage interpreted on seismic data. Mar. Pet. Geol. 26, 1304–1319. https://doi.org/10.1016/j.marpetgeo.2008.09.008.

Løseth, H., Wensaas, L., Arntsen, B., Hanken, N.M., Basire, C., Graue, K., 2011. 1000 M Long Gas Blow-Out Pipes. Mar. Pet. Geol. 28 (5), 1040–1060. https://doi.org/10.

1016/j.marpetgeo.2010.10.001.
Marfurt, K.J., Alves, T.M., 2014. Pitfalls and limitations in seismic attribute interpretation of tectonic features. Interpretation 3 (1), SB5–SB15. https://doi.org/10.1190/INT-2014-0122.1. Retrieved from.
Masoumi, S., Reuning, L., Back, S., Sandrin, A., Kukla, P.A., 2014. Buried pockmarks on the Top Chalk surface of the Danish North Sea and their potential significance for interpreting palaeocirculation patterns. Int. J. Earth Sci. 103 (2), 563–578. https://doi.org/10.1007/s00531-013-0977-2.
Milton-Worssell, R., Smith, K., McGrandle, A., Watson, J., Cameron, D., 2010. The search for a carboniferous petroleum system beneath the Central North Sea. Petroleum geology: from mature basins to New frontiers. Proceedings of the 7th Petroleum *Geology Conference* 7, 57–75. https://doi.org/10.1144/0070057.
Monaghan, A.A., Arsenikos, S., Quinn, M.F., Johnson, K.R., Vincent, C.J., Vane, C.H., Kim, A.W., Uguna, C.N., Hannis, S.D., Gent, C.M.A., Millward, D., Kearsey, T.I., Williamson, J.P., 2017. Carboniferous petroleum systems around the Mid North Sea High, UK. Mar. Pet. Geol. 88, 282–302. https://doi.org/10.1016/j.marpetgeo.2017.08. 019.
Moss, J.L., Cartwright, J., 2010. 3D seismic expression of km-scale fluid escape pipes from offshore Namibia. Basin Res. 22 (4), 481–501. https://doi.org/10.1111/j.1365-2117.2010.00461.x.
Nogues, J.P., Court, B., Dobossy, M., Nordbotten, J.M., Celia, M.A., 2012. A methodology to estimate maximum probable leakage along old wells in a geological sequestration operation. Int. J. Greenh. Gas Control. 7, 39–47. https://doi.org/10.1016/j.ijggc.2011.12.003.
Omosanya, K.O., Alves, T.M., 2013. A 3-dimensional seismic method to assess the provenance of Mass-Transport Deposits (MTDs) on salt-rich continental slopes (Espírito Santo Basin, SE Brazil). Mar. Pet. Geol. 44, 223–239. https://doi.org/10.1016/j.marpetgeo.2013.02.006.
Penge, J., Taylor, B., Huckerby, J., Munns, J., 1993. Extension and salt tectonics in the East Central graben. Petroleum geology of Northwest Europe. Proceedings of the 4th Conference 1197–1209. https://doi.org/10.1007/BF00171455.
Pepper, A.S., Corvit, P.J., 1995. Simple Kinetic Models of Petroleum Formation. Part I : oil and gas generation from kerogen 12 (3), 291–319.
Rattey, R.P., Hayward, A.B., 1993. Sequence stratigraphy of a failed rift system: the Middle jurassic to early cretaceous basin evolution of the Central and Northern North Sea. Petroleum geology of Northwest Europe. Proceedings of the 4th Conference on Petroleum Geology of NW. Europe, at the Barbican Centre 1, 215–249.
Salisbury, R.S.K., 1990. Shallow gas reservoirs and migration paths Over a Central North Sea diapir. Ardus, D.A., Green, C.D. (Eds.), Safety in Offshore Drilling: The Role of Shallow Gas Surveys, Proceedings of an International Conference (Safety in Offshore Drilling) Organized by the Society for Underwater Technology and Held in London, U.K., April 25 {&} 26, 1990 (Pp. 167–180). https://doi.org/10.1007/978-94-009-0669-3_8.
Smith, R.I., Hodgson, N., Fulton, M., 1993. Salt control on Triassic Reservoir distribution, UKCS Central North Sea. Petroleum Geology of Northwest Europe: Proceedings of the 4th Conference. pp. 547–557.
Strozyk, F., Reuning, L., Back, S., Kukla, P., 2018. Giant pockmark formation from cretaceous hydrocarbon expulsion in the western Lower Saxony Basin, the Netherlands. In: Kilhams, B., Kukla, P.A., Mazur, S., McKie, T., Mijnlieff, H.F., van Ojik, K. (Eds.), Mesozoic Resource Potential in the Southern Permian Basin. Geological Society, London, Special Publications, pp. 469.
Thomas, S., 2008. Enhanced oil recovery - an overview. Oil & Gas Science and Technology-Revue 63 (1), 9–19. https://doi.org/10.2516/ogst.
Underhill, J.R., 2003. The tectonic and stratigraphic framework of the United Kingdom's oil and gas fields. Geol. Soc. London Mem. 20 (1), 17–59.
Underhill, J.R., Partington, M.A., 1993. Jurassic thermal doming and deflation in the North Sea: implications of the sequence stratigraphic evidence. Petroleum Geology of Northwest Europe: Proceedings of the 4th Conference on Petroleum Geology of NW. Europe, at the Barbican Centre 1, 337–345.
Wagner, B.H., Jackson, M.P.A., 2011. Viscous flow during salt welding. Tectonophysics 510 (3–4), 309–326. https://doi.org/10.1016/j.tecto.2011.07.012.
Wilkinson, M., Haszeldine, R.S., Mackay, E., Smith, K., Sargeant, S., 2013. A new stratigraphic trap for CO_2 in the UK North Sea: Appraisal using legacy information. Int. J. Greenh. Gas Control. 12, 310–322. https://doi.org/10.1016/j.ijggc.2012.09.013.
Williams, J.D.O., Jin, M., Bentham, M., Pickup, G.E., Hannis, S.D., Mackay, E.J., 2013. Modelling carbon dioxide storage within closed structures in the UK Bunter Sandstone Formation. Int. J. Greenh. Gas Control. 18, 38–50. https://doi.org/10.1016/j.ijggc.2013.06.015.
Xia, C., Wilkinson, M., 2017. The geological risks of exploring for a CO 2 storage reservoir. Int. J. Greenh. Gas Control. 63 (July), 272–280. https://doi.org/10.1016/j.ijggc.2017.05.016.
Zanella, E., Coward, M.P., 2003. Structural framework. In: Evans, D., Graham, C., Armour, A., Bathurst, P. (Eds.), The Millennium Atlas: Petroleum Geology of the Central and Northern North Sea. The Geological Society, London, pp. 45–59.
Ziegler, P., 1992. North sea rift system. Tectonophysics 208, 55–75.